CZECH UNIVERSITY OF LIFE SCIENCES PRAGUE

FACULTY OF ENVIRONMENTAL SCIENCES

DEPARTMENT OF ENVIRONMENTAL GEOSCIENCES

STUDY OF CONTAMINATION WITH POLY- AND PERFLUOROALKYL SUBSTANCES IN THE ARCTIC REGION

DIPLOMA THESIS

THESIS SUPERVISOR: ING. BARBORA BÖSERLE HUDCOVÁ, PH.D.

AUTHOR: B.Sc. ASWATHI GOPINATH

2026

CZECH UNIVERSITY OF LIFE SCIENCES PRAGUE

Faculty of Environmental Sciences

DIPLOMA THESIS ASSIGNMENT

B.Sc. Aswathi Gopinath

Environmental Geosciences

Thesis title

Study of contamination with poly- and perfluoroalkyl substances in the Arctic region

---

Objectives of thesis

The aim of the thesis will be to summarize the sources, risks, and contamination levels of poly- and perfluoroalkyl substances (PFAS) in the Arctic with a special emphasis on the Svalbard region. The work will also include a description of various PFAS sampling methods, particularly using the DGT (Diffusive Gradients in Thin Films) technique. Although the use of DGT samplers for PFAS is still limited, they have proven to be an efficient tool for determining labile forms of elements in surface waters, soils, and sediments. The review part of the thesis will cover general contamination in the Arctic region (especially focused on the Svalbard region), detailed information about PFAS (classification, sources, risks, mobility, and bioaccumulation), and various sampling methods and analytical techniques for studying PFAS contamination. In the experimental part, samples collected from Svalbard, especially using DGT samplers, will be processed to assess PFAS contamination in this area. The obtained results will be analyzed, summarized, and discussed in detail.

Methodology

The first part of the thesis will be devoted to a thorough literature review based on the recommended and searched literature. The literature review will focus on three main topics: 1) Contaminants in the Arctic regions with a special focus on Svalbard region – basic classification of contaminants, sources, and associated risks, 2) Forever chemicals in the environment – basic classification, occurrence, mobility, and bioaccumulation, 3) Sampling methods and analytical techniques for PFAS – principles, applications, and limitations. The experimental part of the thesis will focus on the processing of samples collected from Svalbard, particularly those obtained using DGT samplers. This section will be divided into: 1) Methodology of experiments and analyses, 2) Obtained results, 3) Discussion of the results. The preparation of the thesis will follow the Methodological Guidelines for writing Diploma Thesis at the FZP, Czech University of Life Sciences Prague.

The proposed extent of the thesis

40-50

Keywords

poly- and perfluoroalkyl substances, forever chemicals, contamination, Arctic region, DGT samplers

---

Recommended information sources

Alam, M.S., Abbasi, A., Chen G., 2024. Fate, distribution, and transport dynamics of Per- and Polyfluoroalkyl Substances (PFASs) in the environment. J. Environ. Manage. 371, 123163.

Brennan, N.M., Evans, A.T., Fritz, M.K., Peak, S.A.,von Holst, E., 2021. Trends in the Regulation of Per- and Polyfluoroalkyl Substances (PFAS): A Scoping Review. Int. J. Environ. Res. Public Health 18, 10900.

Fang, Z., Li, Y., Li, Y., Yang, D., Zhang, H., Jones, K.C., Gu, C., Luo, J., 2021. Development and Applications of Novel DGT Passive Samplers for Measuring 12 Per- and Polyfluoroalkyl Substances in Natural Waters and Wastewaters. Environ. Sci. Technol. 55(14), 9548–9556.

Hartz, W.F., Björnsdotter, M.K., Yeung, L.W.Y., Humby, J.D., Eckhardt, S., Evangeliou, N., Jogsten, I.E., Kärrman, A., Kallenborn, R., 2024. Sources and Seasonal Variations of Per- and Polyfluoroalkyl Substances (PFAS) in Surface Snow in the Arctic. Environ. Sci. Technol., 58(49), 21817–21828.

Lyu, X., Xiao, F., Shen, C., Chen, J., Park, C.M., Sun, Y., Flury, M., Wang, D., 2022. Per- and Polyfluoroalkyl Substances (PFAS) in Subsurface Environments: Occurrence, Fate, Transport, and Research Prospect. Rev. Geophys. 60, e2021RG000765.

Stroski, K.M., Luong, K.H., Challis, J.K., Chaves-Barquero, L.G., Hanson, M.L., Wong, C.S., 2020. Wastewater sources of per- and polyfluorinated alkyl substances (PFAS) and pharmaceuticals in four Canadian Arctic communities. Sci. Total Environ. 708, 134494.

Wang, P., Challis, J.K., Luong, K.H., Vera, T.C., Wong, C.S., 2021. Calibration of organic-diffusive gradients in thin films (o-DGT) passive samplers for perfluorinated alkyl acids in water. Chemosphere 263, 128325.

Yang, Y., Liu, S., Wang, R., Li, C., Tang, J., Chen, T., Ying, G.-G., Chen C.-E., 2022. Diffusive gradients in thin films (DGT) probe for effectively sampling of per- and polyfluoroalkyl substances in waters and sediments. J. Environ. Sci. 121, 90-97.

Zhang, J., Hu, L., Xu, H., 2024. Dietary exposure to per- and polyfluoroalkyl substances: Potential health impacts on human liver. Sci. Total Environ. 907, 167945.

Expected date of thesis defence

2025/26 LS – FZP

Thesis supervisor

Ing. Barbora Böserle Hudcová, Ph.D.

Supervising department

Department of Environmental Geosciences

Electronic approval: 22. 08. 2025

prof. RNDr. Vladislav Chrastný, Ph.D.

Head of department

Electronic approval: 27. 08. 2025

prof. RNDr. Michael Komárek, Ph.D.

Dean

Prague on 26. 03. 2026

Author's statement

I hereby declare that I have independently elaborated the diploma thesis with the topic of Study of contamination with poly- and perfluoroalkyl substances in the Arctic region and that I have cited all the information sources that I used in the thesis and that are also listed at the end of the thesis in the list of used information sources.

I am aware that my diploma thesis is subject to Act No. 121/2000 Coll., on copyright, on rights related to copyright and on amendment of some acts, as amended by later regulations, particularly the provisions of Section 35(3) of the act on the use of the thesis.

I am aware that by submitting the diploma thesis I agree with its publication under Act No.111/1998 Coll., on universities and on the change and amendments of some acts, as amended, regardless of the result of its defence.

With my own signature, I also declare that the electronic version is identical to the printed Version and the data stated in the thesis has been processed in relation to the GDPR.

In Prague, on 30 March 2026 ……

B.S.c. Aswathi Gopinath

Acknowledgement

I would like to express my sincere gratitude to the Department of Environmental Sciences for giving me the opportunity to undertake this thesis. I am especially thankful to my thesis supervisor, Ing. Barbora Böserle Hudcová, Ph.D., for her continuous support, guidance, and valuable insights throughout the completion of this work. I would also like to thank Ing. Šárka Lewandowská for her assistance during the laboratory work and in the analysis of results.

I would also like to thank my professors and colleagues at the university for their encouragement and for motivating me to put in my best effort.

I am deeply grateful to Ananthu Suresh, my boyfriend, for being a constant source of strength and for his emotional support throughout this journey. Finally, I would like to thank my family for their unwavering belief in me.

ABSTRACT

This study investigated PFAS contamination at two contrasting sites near Longyearbyen, close to Svalbard Airport (an AFFF-impacted coastal plain with an active remediation programme), and the municipal wastewater outfall in Adventfjorden. To study time-weighted average dissolved PFAS concentrations, diffusive gradients in thin films (DGT; LSNW-AP) and polar organic chemical integrative samplers (POCIS; PFAS-specific and HLB configurations) were deployed for 30-35 days at both. Moreover, sediment samples from the airport site were also analyzed. Prior to field application, laboratory testing revealed acceptable DGT recoveries for PFBA (82%) and PFOA (94%) in freshwater, while PFOS showed reduced recovery in seawater (19%), indicating compound- and matrix-specific limitations, especially in closed batch systems. In the field, eleven types of PFAS were detected at the airport site by DGT, with a summed mean concentration of 63.08 ± 15.81 ng/L, dominated by PFHxS (16.22 ng/L), PFHxA (15.22 ng/L), and PFPeA (13.23 ng/L). POCIS-PFAS yielded a comparable total of 53.94 ± 3.39 ng/L with a similar compound profile, while POCIS-HLB returned higher summed concentrations (125.17 ± 16.04 ng/L) dominated by PFHxS, PFHpA, PFPeA, and PFOA, though with a less representative profile for short-chain PFAS. No PFAS were detected at the wastewater site by any sampler. Sediment analysis identified PFOS as the dominant compound (mean 0.45 ± 0.13 ng/g dw), followed by PFNA and PFHxS, consistent with an AFFF contamination signature. The results confirm that PFAS contamination at Svalbard Airport is driven by AFFF-related local sources, with a mixed dissolved profile of sulfonates and mid-chain perfluorocarboxylates in the water and preferential enrichment of long-chain sulfonates in sediment. The close agreement between DGT and POCIS-PFAS supports the use of DGT as a complementary passive sampling tool in cold Arctic waters, despite possible compound- and matrix-specific limitations. The study provides baseline data for remediation progress monitoring and for the further development of passive sampling in remote polar environments.

Keywords:

Poly- and perfluoroalkyl substances, forever chemicals, contamination, Arctic region, DGT samplers.

ABSTRAKT

Tato studie zkoumala kontaminaci PFAS na dvou kontrastních lokalitách poblíž Longyearbyenu, blízko letiště na Špicberkách (pobřežní nížina ovlivněná AFFF s aktivním sanačním programem), a na vypouštění městských odpadních vod v Adventfjorden. Pro studium časově vážených průměrných koncentrací rozpuštěných PFAS byly na obou po dobu 30–35 dnů nasazeny difuzní gradienty v tenkých vrstvách (DGT; LSNW-AP) a integrační vzorkovače polárních organických chemikálií (POCIS; konfigurace specifické pro PFAS a HLB). Dále byly analyzovány také vzorky sedimentů z lokality letiště. Před aplikací v terénu laboratorní testy ukázaly přijatelné výtěžnosti DGT pro PFBA (82 %) a PFOA (94 %) ve sladké vodě, zatímco PFOS vykazovaly sníženou výtěžnost v mořské vodě (19 %), což naznačuje omezení specifická pro danou sloučeninu a matrici, zejména v uzavřených dávkových systémech. V terénu bylo na letišti detekováno jedenáct typů PFAS pomocí DGT s celkovou průměrnou koncentrací 63,08 ± 15,81 ng/l, kde dominovaly PFHxS (16,22 ng/l), PFHxA (15,22 ng/l) a PFPeA (13,23 ng/l). POCIS-PFAS vykázala srovnatelný celkový počet 53,94 ± 3,39 ng/l s podobným profilem sloučenin, zatímco POCIS-HLB vykázala vyšší souhrnné koncentrace (125,17 ± 16,04 ng/l), kde dominovaly PFHxS, PFHpA, PFPeA a PFOA, ačkoli s méně reprezentativním profilem pro PFAS s krátkým řetězcem. V místě výpusti odpadních vod nebyly žádným vzorkovačem detekovány žádné PFAS. Analýza sedimentů identifikovala PFOS jako dominantní sloučeninu (průměr 0,45 ± 0,13 ng/g suché hmotnosti), následovanou PFNA a PFHxS, což je v souladu s typem kontaminace AFFF. Výsledky potvrzují, že kontaminace PFAS na letišti na Špicberkách je způsobena místními zdroji souvisejícími s AFFF, se smíšeným profilem rozpuštěných sulfonátů a perfluorkarboxylátů se střední částí řetězce ve vodě a preferenčním obohacením sedimentů o sulfonáty s dlouhým řetězcem. Úzká shoda mezi DGT a POCIS-PFAS podporuje použití DGT jako doplňkového nástroje pro pasivní vzorkování v chladných arktických vodách, a to navzdory možným omezením specifickým pro dané sloučeniny a matrici. Studie poskytuje základní data pro monitorování pokroku v sanaci a pro další rozvoj pasivního vzorkování ve vzdálených polárních prostředích.

Klíčová slova:

Poly- a perfluoralkylované látky, chemikálie Forever, kontaminace, arktická oblast, vzorkovače DGT.

TABLE OF CONTENTS

1. Introduction…….. 1

2. Objectives of the thesis…… 3

3. Literature review…… 4

3.1. Contaminants in the Arctic Region…….. 4

3.2. Inorganic pollutants…….. 4

3.2.1. Sources and transport pathways…… 5

3.2.2. Distribution in the environment…… 6

3.3. Persistent organic pollutants…… 7

3.3.1. Sources and transport pathways……... 8

3.3.2. Transport mechanisms…….. 8

3.4. Per- and polyfluoroalkyl Substances (Forever Chemicals)…… 10

3.4.1. Sources, Production and Transport of PFAS…… 12

3.4.2. PFAS Life Cycle Emissions…… 13

3.4.3. Long-Range Transport to the Arctic…… 14

3.4.4. PFAS Accumulation in Different Environments…… 15

3.4.4.1. PFAS in Terrestrial Biota…….. 17

3.4.4.2. PFAS in Freshwaters…… 17

3.5. Arctic as Sink and Source…… 18

3.6. Methods for Sampling Soil and Water Contaminated with PFAS…….. 19

3.6.1. Grab Sampling……..20

3.6.2. Passive Sampling…….. ……..21

3.6.2.1. POCIS……... 21

3.6.2.2. DGT…….. 23

3.7. PFAS Analytical Methods…….. 25

4. Methodology…….. 26

4.1. Description of The Study Area…… 26

4.2. Sampling Sites…… 27

4.3. Sample Collection……27

4.4. Preliminary testing of DGT samplers in a laboratory environment……28

4.5. Passive Samplers from the field……...30
4.5.1. DGT PFAS Extraction……..30
4.5.2. POCIS Extraction…… 33
4.6. PFAS Analysis in the Sediment…….. 35
4.7. Instrumental method for PFAS Analysis…… 35
4.8. Elemental Water analysis and Sediment digestion…… 35

5. Results…… 37
5.1. General Characteristics of Water…… 37
5.2. General Characteristics of Sediment……39
5.2.1. Major Elements……39
5.2.2. Trace Metals and Metalloids and Selected Non-metals…….....40
5.3. Laboratory Testing of DGT (Freshwater and Seawater)……42
5.4. Passive Samplers from the field……..… 46
5.4.1. DGT……..46
5.4.2. POCIS-PFAS Sampler…… 48
5.4.3. POCIS-HLB Sampler…….. 49
5.4.4. Summary of Passive Samplers Results…… 50
5.5. PFAS Sediments…… 51

6. Discussion…… 53
6.1. Laboratory Testing of DGT……53
6.2. Field Passive Samplers……54
6.2.1. Comparison of DGT and POCIS-PFAS……..…… 56
6.3. PFAS Sediments…… 56

7. Conclusion…… 59

8. Bibliography and Sources used…….. 60

1. INTRODUCTION

The Arctic environment, despite its remoteness from major centers of industrial activity, has emerged as one of the most sensitive indicators of global anthropogenic contamination. Through long-range atmospheric and oceanic transport, pollutants originating from lower latitudes accumulate in polar regions, making the Arctic both a barometer of global contamination pressures and a repository for decades of chemical emissions (AMAP, 2017; Lohmann et al., 2023). Among the contaminants of greatest current concern, per- and polyfluoroalkyl substances (PFAS) stand out due to their extraordinary environmental persistence, bioaccumulation potential, and capacity for long-range transport (Zhou et al., 2023). The strength of the carbon-fluorine bond renders PFAS resistant to all known natural degradation pathways, earning them the designation of "forever chemicals" and they are now detected ubiquitously across all environmental compartments, including the most remote Arctic systems (Buck et al., 2011; AMAP, 2017).

The Svalbard archipelago represents a particularly compelling study system for PFAS research, as it is subject to both diffuse background inputs from long-range transport and locally intensified contamination from the settlement infrastructure of Longyearbyen, including wastewater discharge, airport operations, and a history of firefighting training using aqueous film-forming foam (AFFF), one of the most significant point sources of PFAS contamination globally (Skaar et al., 2019; Kwok et al., 2013). Previous studies have documented elevated PFAS concentrations near Longyearbyen relative to remote reference sites, confirming a clear superimposition of local sources on background deposition signals (Kwok et al., 2013; Arulananthan et al., 2025). Climate change further complicates this picture: thawing permafrost and melting glaciers are increasingly releasing historically accumulated PFAS back into aquatic systems, potentially shifting the Arctic from a net sink to a secondary source (Ahrens et al., 2011; AMAP, 2017).

Monitoring PFAS in Arctic waters presents considerable analytical challenges. PFAS occur across a wide concentration range, from sub-ng/L in pristine waters to µg/L near point sources, and conventional grab sampling captures only an instantaneous snapshot, poorly representing time-averaged exposure relevant to ecological risk assessment (Arulananthan et al., 2025; AMAP, 2017). Passive sampling techniques, including diffusive gradients in thin films (DGT) and polar organic chemical integrative samplers (POCIS), overcome these limitations by accumulating analytes over extended deployment periods to yield time-weighted average (TWA) concentrations, and offer practical advantages for remote field deployment (Hale et al., 2021). Despite these merits, their comparative performance across the contrasting salinities and temperatures encountered in Arctic coastal environments from glacially influenced freshwater to fjord water remains insufficiently characterized.

Given the ecological sensitivity of the Arctic, the ongoing expansion of human infrastructure in Svalbard, and the accelerating influence of climate change on contaminant remobilization, there is a clear and pressing need for robust, time-integrated assessments of PFAS contamination in this region. Such studies are essential for understanding the relative contributions of local and long-range sources, evaluating the suitability of emerging passive sampling tools under Arctic conditions, and informing future monitoring frameworks and environmental protection strategies.

2. OBJECTIVES OF THE THESIS

The aim of the thesis will be to summarize the sources, risks, and contamination levels of poly- and perfluoroalkyl substances (PFAS) in the Arctic with a special emphasis on the Svalbard region. The work will also include a description of various PFAS sampling methods, particularly using the DGT (Diffusive Gradients in Thin Films) technique. Although the use of DGT samplers for PFAS is still limited, they have proven to be an efficient tool for determining labile forms of elements in surface waters, soils, and sediments. The review part of the thesis will cover general contamination in the Arctic region (especially focused on the Svalbard region), detailed information about PFAS (classification, sources, risks, mobility, and bioaccumulation), and various sampling methods and analytical techniques for studying PFAS contamination. In the experimental part, samples collected from Svalbard, especially using DGT samplers, will be processed to assess PFAS contamination in this area. The obtained results will be analyzed, summarized, and discussed in detail.

3. LITERATURE REVIEW

3.1 Contaminants in the Arctic Region

The Arctic environment, despite its remoteness and limited local industrial activity, functions as a global sink for anthropogenic contaminants transported from lower latitudes (Lohmann et al., 2023, 2024). These contaminants reach the polar region via complex long-range atmospheric and oceanic transport pathways (Dunn et al., 2024). Once deposited, they undergo cold-region specific cycling processes, including cold condensation and trapping in snow and ice, which promote their retention and entry into Arctic food webs (Roos et al., 2022).

Organic contaminants in the Arctic comprise legacy persistent organic pollutants (POPs) such as polychlorinated biphenyls (PCBs) and organochlorine pesticides (e.g., DDT), as well as a growing suite of current-use and emerging compounds. These substances are typically semi-volatile, hydrophobic, and resistant to degradation, which facilitates their long-range transport and bioaccumulation in biota (AMAP, 2017). Among the newer classes of contaminants, per- and polyfluoroalkyl substances (PFAS) have attracted particular attention due to their extreme environmental persistence, bioaccumulation potential, and capacity for long-range transport to remote polar environments (Zhou et al., 2026).

Inorganic contaminants include potentially toxic metals and metalloids such as mercury (Hg), lead (Pb), cadmium (Cd), and arsenic (As), which originate from both natural geological processes and anthropogenic activities (Zhou et al., 2024; AMAP, 2017). The interaction between these contaminants and the fragile Arctic environment requires a clear understanding of their specific chemical behaviors, transport efficiencies, and ecological impacts.

3.2 Inorganic Pollutants

The dominant inorganic contaminants in the Arctic are potentially toxic metals and metalloids, including Hg, Pb, Cd, and As, along with anthropogenic radionuclides such as ^{137}Cs, ^{238}Pu, $^{239+240}Pu$, and ^{241}Am (AMAP, 2017; Gwynn et al., 2016). These elements pose substantial environmental risks due to their persistence, bioaccumulation, and potential to bio magnify through Arctic food webs. Recent studies in Svalbard and other Arctic regions report elevated concentrations of Cd, Hg, and Pb in some soils and sediments, particularly near human-impacted sites (AMAP, 2017).

Anthropogenic activities, including coal and metal mining, fossil-fuel combustion, industrial emissions, and other human activities, are the main sources of these metals to the Arctic (AMAP, 2017). Natural inputs arise from rock weathering, sea-salt, dust aerosols, and episodic volcanic activity (Zdanowicz et al., 2013).

3.2.1 Sources and Transport Pathways

Long Range Atmospheric Transport

Atmospheric processes act as the dominant pathway for inorganic pollutants to enter the Arctic. As a result of global circulation patterns, pollutants from lower latitudes are deposited into the Arctic mainly through wet and dry deposition processes, establishing long-range atmospheric transport as the most significant mechanism (AMAP, 2017) (Fig 1).

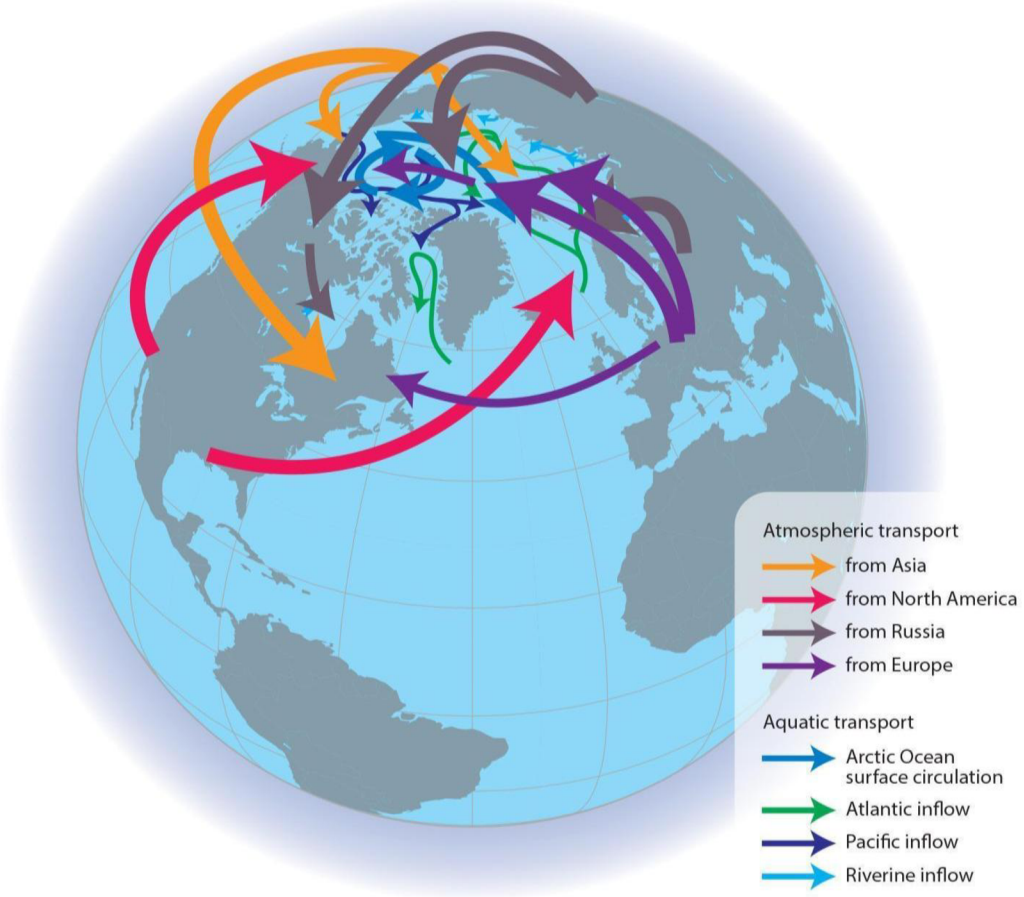

Fig 1: Sources of long-range transport to the arctic (AMAP, 2013).

Mercury is widely studied and is found to be highly deposited by long-range transport, especially during Atmospheric Mercury Depletion Events (AMDEs) that occur during polar spring in the Arctic, which contribute approximately 50 to 300 tonnes of mercury deposition per annual cycle (AMAP, 2017). Lead contamination is also primarily a result of long-range atmospheric transport. Analysis of Greenland ice cores reveals evidence for long-range transport and deposition of cadmium, lead, and thallium, with concentrations increasing by approximately 10-fold due to industrial activities compared to pre-industrial baselines (McConnell & Edwards, 2008). Analysis of

Arctic snow samples also shows elevated concentrations of lead isotopes characteristic of coal and fuel combustion (Zdanowicz et al., 2013).

Local and Regional Transport

In addition to long-range inputs, local and regional sources can create contamination hotspots in parts of the Arctic, especially near settlements, mining and industrial areas, ports, and military installations (AMAP, 2017; Muir et al., 2025). At populated sites in Svalbard, soils and near-shore sediments show locally elevated concentrations of potentially toxic metals compared with surrounding background areas, reflecting inputs from historical coal mining, fuel handling, waste disposal, and shipping activities (Gulińska et al., 2003). These local contamination signals tend to dissipate within hundreds of meters, and natural variability related to bedrock geology often dominates at larger spatial scales. Marine sediments in fjords and near shipping lanes also exhibit higher contaminant levels, indicating contributions from local marine traffic and coastal infrastructure (AMAP, 2017).

Mining activities serve as an important source of local pollution, particularly leading to elevated lead concentrations. Evidence of mining-related contamination has been documented in the Siberian Arctic, particularly on the Taimyr Peninsula (AMAP, 2017).

Secondary Sources and Remobilization

Another rising concern in the Arctic region is secondary contamination, including the remobilization of contaminants previously deposited and stored in cryospheric reservoirs. In Svalbard, melting glaciers and thawing permafrost are important contributors to secondary pollution (AMAP, 2017). Recent studies have shown increases in metal concentrations in organic soils and marine sediments linked to meltwater inputs (Zdanowicz et al., 2013). Volcanic eruptions are also periodic natural sources of metal contamination in the Arctic (AMAP, 2017).

3.2.2 Distribution in Environment

Terrestrial Systems

The distribution of inorganic contaminants in terrestrial systems is governed primarily by bedrock geology, soil organic matter content, proximity to anthropogenic sources, and cryoturbation processes that mix surface and subsurface soil horizons (AMAP, 2017). In the Norwegian Arctic, surface soils contain mercury and other metals at trace concentrations, largely reflecting natural geochemical baselines with localized anthropogenic enrichment near settlements (Ottesen et al., 2001).

Marine and Aquatic Systems

Marine and aquatic systems function as both sinks and sources of inorganic contaminants, with concentrations varying along hydrological pathways depending on

watershed characteristics, depositional environments, and anthropogenic inputs (AMAP, 2017). In Svalbard fjord sediments, aluminum, lead, manganese, chromium, and molybdenum exhibited the highest enrichment factors relative to geochemical baselines (Zaborska et al., 2017).

Cryosphere

The Arctic cryosphere, including snow, ice, glaciers, and permafrost, plays a major role in contaminant cycling by acting as long-term storage reservoirs that release accumulated contaminants in response to warming-induced melting and thaw (AMAP, 2017; Zdanowicz et al., 2013).

3.3 Persistent Organic Pollutants

Persistent organic pollutants (POPs) are defined as a group of organic pollutants that are resistant to natural degradation. They persist in the environment for years to decades, bioaccumulate in the food chain, cause serious health impacts, and are subject to long-range atmospheric transport (Stockholm Convention, 2001; AMAP, 2017).

The Stockholm Convention has sought to eradicate the release of POPs into the environment, taking into consideration their hazardous properties. POPs are categorized as "legacy POPs" and "emerging POPs" based on their occurrence history and regulatory status. Legacy POPs are those pollutants that have existed in the environment for decades and are already subject to international restrictions and regulations. Legacy POPs include polychlorinated biphenyls (PCBs), 1,1,1-trichloro-2,2-bis(4-chlorophenyl) ethane (DDT), hexachlorobenzene (HCB), and many other organochlorine compounds (Stockholm Convention, 2001). Most legacy POPs have been banned for years, leading to substantial decreases in their environmental concentrations (AMAP, 2017).

Emerging POPs represent a heterogeneous group; while some, such as perfluorooctanoic acid (PFOA) and perfluorooctane sulfonate (PFOS), as the most common PFAS representatives, are now listed under the Stockholm Convention and subject to international restrictions. However, many other emerging contaminants have not yet been regulated globally (Stockholm Convention, 2019; AMAP, 2017). The term "emerging" does not refer to substances that are new to the environment, but rather to those that have only recently come to scientific and regulatory attention, often as a result of advances in analytical detection capabilities and a growing understanding of their long-term environmental risks and health effects (Muir et al., 2025; AMAP, 2017). Many emerging POPs, including PFAS, have been present in the environment and used industrially for several decades but were not detected or assessed as contaminants of concern until analytical methods became sufficiently sensitive (Arulananthan et al., 2025).

In most parts of the Arctic, the majority of detected contaminants lack a direct local, providing clear evidence of long-range transport across hemispheric scales (AMAP,

2017; Muir et al., 2025). However, in areas such as Svalbard, where human settlements, mining operations, and tourism infrastructure exist, local sources may also contribute to contamination burdens and should not be overlooked (Gulińska et al., 2003; Arulananthan et al., 2025).

3.3.1 Sources and Transport Pathways

Due to the remote location and sparse population in the Arctic, the primary sources of POPs are located in distant industrial and agricultural areas at lower latitudes. In some cases, however, local sources can be identified. For instance, inefficient wastewater treatment plants may release pharmaceuticals and chemicals used in personal care and household products. These concerns can be mitigated by improving the efficiency of wastewater treatment infrastructure in these areas (Muir et al., 2025).

Some current-use contaminants being studied as potential emerging POPs may exhibit shorter environmental half-lives under optimal conditions; however, in the Arctic, low temperatures substantially reduce biodegradation and photolysis rates, extending the environmental persistence of compounds with moderate degradability (Muir et al., 2025). Consequently, even compounds not classically defined as POPs can accumulate in the Arctic environment if inputs are sustained.

3.3.2 Transport Mechanisms

The long-range transport of POPs to the Arctic occurs primarily through atmospheric pathways, with additional contributions from oceanic currents. Semi-volatile POPs undergo repeated cycles of volatilization, atmospheric transport, and re-deposition; a process known as the "grasshopper effect" which progressively moves these compounds from warmer source regions toward cooler polar areas (Wania & Mackay, 1996). More volatile compounds such as hexachlorocyclohexanes (HCHs) and hexachlorobenzene (HCB) are transported more efficiently and in greater quantities, while less volatile higher-chlorinated PCBs travel shorter distances and deposit closer to their emission sources (AMAP, 2017). In addition to atmospheric transport, oceanic currents carry dissolved and particle-bound POPs to the Arctic Ocean, where they partition into sediments and biota (AMAP, 2017).

Before 2000, due to high levels of industrial and agricultural activities, Europe and North America were responsible for the majority of POP emissions to the atmosphere. However, as new regulations are being imposed, the origin of these pollutants has shifted to emerging or developing regions in Asia (AMAP, 2017; Muir et al., 2025). Glaciers serve as long-term storage reservoirs for POPs, and due to climate change, when glaciers melt, these pollutants are released back into the environment (AMAP, 2017). Most of the emerging chemicals in the Arctic originate from industries such as textiles, furniture, electronics, personal care products, and pharmaceuticals. Long-range transport is not the only source of POP accumulation; local and regional sources also contribute (Fig 2). The increasing number of tourists visiting the Arctic may also act as potential carriers of contaminants (Muir et al., 2025).

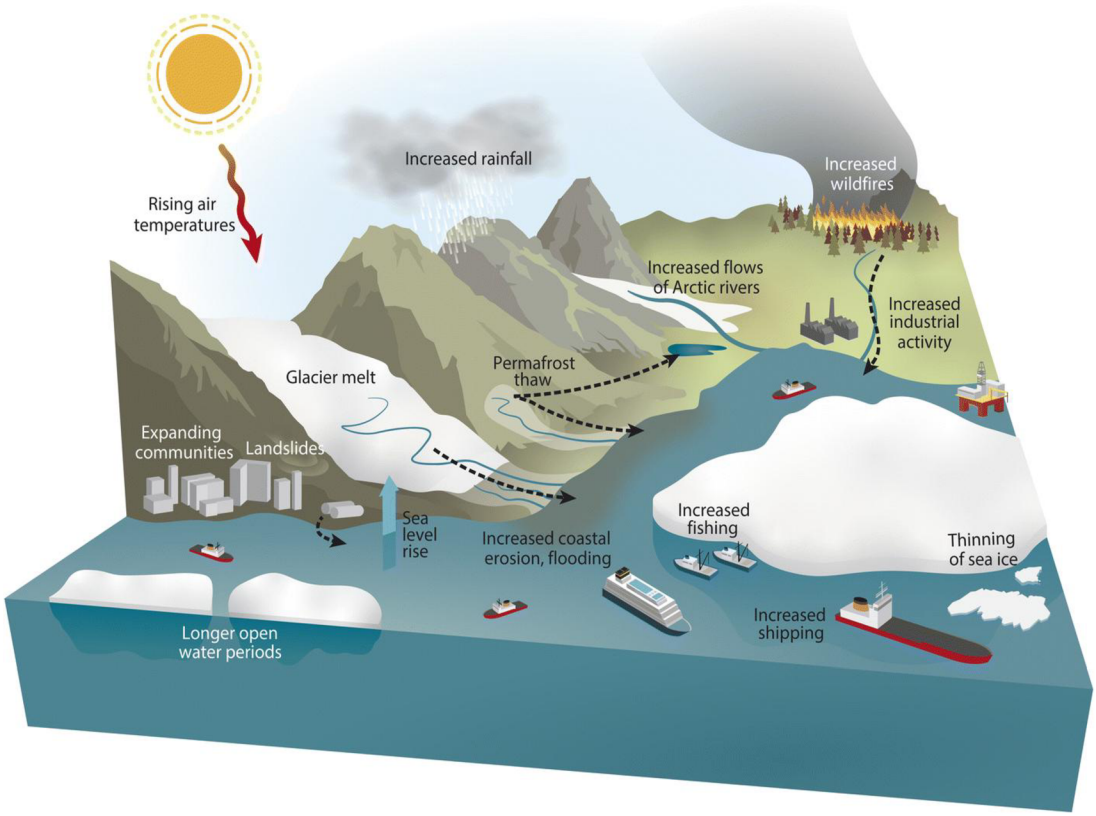

Fig 2: Factors contributing to local and secondary sources of POPs to the arctic (Murir et al, 2024).

The fastest transport of POPs to the Arctic occurs through air, which also acts as a medium for transferring chemicals into food chains. However, many emerging contaminants dissolve more readily in water, indicating that oceanic currents could be a more influential transport pathway for these substances (Muir et al., 2025). Transport of contaminants to and within the Arctic is influenced by weather patterns, geographic location, and the chemical properties of the contaminants and transport media. Parameters such as solubility, volatility, and adsorption capacity affect transport efficiency. POPs are transported through both air and water currents, and some semi-volatile POPs undergo continuous air-water cycling via the "grasshopper effect." Although most transport occurs through air, only a small fraction of pollutants remain airborne, as most are stored in oceans and terrestrial and aquatic environments (AMAP, 2017).

Long-range transport of pollutants to the Arctic is limited in summer, but as high-pressure systems influence the North Atlantic and Eurasian continent in winter, the transport of large amounts of POPs from the continents is favored (AMAP, 2017). A similar seasonal pattern is observed in Antarctica. Some pollutants, such as HCH and HCB, are more volatile and can be transported more quickly and in larger quantities to the Arctic; therefore, their concentrations may be higher in the Arctic than near source regions. Less volatile pollutants, on the other hand, are transported less effectively. Unlike other regions, most depositions in the Arctic occur through snow,

which is capable of scavenging many POPs. However, as snow ages and undergoes metamorphism, it can retain pollutants and subsequently re-release them into the environment (AMAP, 2017).

Among the POPs of greatest current concern are per- and polyfluoroalkyl substances (PFAS), which are widely used in industrial and commercial applications due to their thermal stability and chemical resistance, and are predominantly transported and distributed through aquatic pathways due to their high-water solubility. Their extreme persistence, resulting from the strength of the carbon–fluorine bond, has led to their designation as "forever chemicals" (Buck et al., 2011).

3.4 Per and Polyfluoroalkyl Substances (Forever Chemicals)

Per- and polyfluoroalkyl substances (PFAS) are a large and diverse group of synthetic fluorinated aliphatic compounds characterized by the exceptional strength and stability of the carbon-fluorine (C-F) bond, one of the strongest bonds in organic chemistry (Buck et al., 2011). This property renders most PFAS highly resistant to thermal, chemical, and biological degradation, leading to their designation as "forever chemicals" in both scientific and public discourse (AMAP, 2017). Due to these properties, PFAS are used in a wide range of industrial and commercial applications (Fig 3). In the case of perfluoroalkyl substances, the alkyl chain is fully fluorinated. In contrast, polyfluoroalkyl substances are only partially fluorinated, as they contain at least one carbon atom in the alkyl chain with a hydrogen atom still attached. PFAS are further classified into PFSA (perfluoroalkylsulfonates) and PFCA (perfluorocarboxylates), as well as FTOH (fluorotelomer alcohols) that can act as neutral precursors of PFCAs (Buck et al., 2011; AMAP, 2017). PFAS have varying chain lengths and are distinguished as long-chain (8 or more perfluorinated carbon atoms) and short-chain (7 or fewer perfluorinated carbon atoms) (Buck et al., 2011).

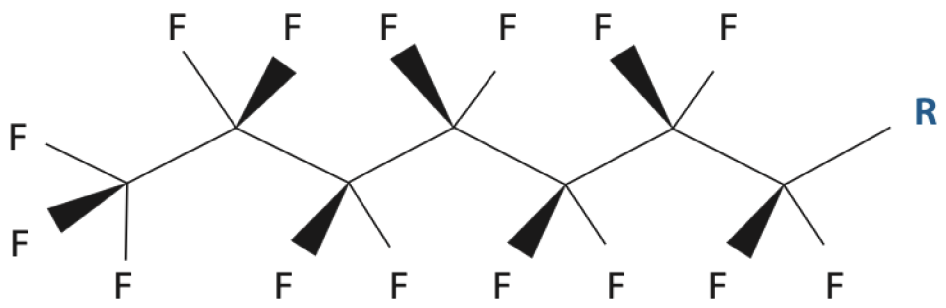

Fig 3: Molecular structure of PFAS (AMAP, 2016)

The production of fully fluorinated carbon compounds began in the late 1800s. The simplest fully fluorinated compound, carbon tetrafluoride (CF_4), was first synthesized in 1886 (Okazoe, 2009). In the mid-twentieth century, as fluorine chemistry advanced,

scientists began to synthesize more complex fluorinated chemicals with different functional groups. These compounds became popular and important due to their excellent thermal stability and resistance to oil, water, stains, and grease (Meegoda et al., 2020).

Polytetrafluoroethylene (PTFE) was discovered in 1938 by DuPont and was later marketed under the name Teflon (Okazoe, 2009). An American company, 3M, began the mass manufacture of fluorinated compounds in the early 1950s using a process called electrochemical fluorination (ECF). This process was used to produce chemicals such as perfluoroalkanesulfonyl fluorides (PASFs) and their derivatives in large quantities. Since the 1960s, other fluorinated polymers such as PVDF (polyvinylidene fluoride) and PVF (polyvinyl fluoride) have also been developed for industrial applications (Okazoe, 2009). From the 1970s onward, a new manufacturing method called telomerization was introduced for industrial purposes, primarily to produce fluorotelomer-based chemicals, which are a type of PFAS (Fig 4). This significantly increased PFAS production (Okazoe, 2009).

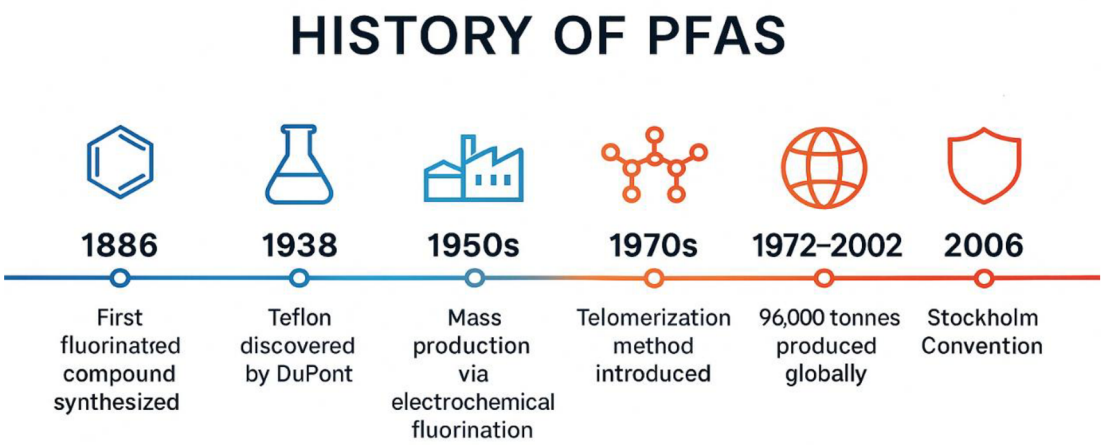

Fig 4: A timeline of major milestones in the historical development of PFAS (Author's own elaboration based on the literature cited in the text; visual layout assisted by Microsoft Copilot).

The occurrence of PFAS in the environment depends on chain length, physical and chemical properties, and functional groups. PFSAs and PFCAs have very low dissociation constants (pKa < 1 for PFSAs and pKa ~0-3.5 for PFCAs), and as a result, they exist in their fully ionized forms in most environmental conditions (Buck et al., 2011). They are found to bind to proteins and phospholipid tissues such as the liver and kidneys. Some PFAS bioaccumulate in food webs and are toxic (AMAP, 2017). The distribution, partitioning, and accumulation of PFAS in abiotic environments are controlled by their chain length and functional groups. For PFCAs and PFSAs, the

organic carbon partition coefficient (log K_{OC}) is relatively lower (approximately 1.3 to 3.5) compared to neutral organohalogens (Buck et al., 2011). Short-chain PFAS are predominantly found in dissolved form and persist longer in aquatic environments, potentially facilitating long-range aquatic transport. Long-chain PFAS binds more strongly to particles depending on organic carbon content, pH, and the presence of metal ions. These factors play an important role in determining their transport across various environments (AMAP, 2017; Buck et al., 2011).

3.4.1 Sources, Production, and Transport of PFAS

PFAS have been produced since the 1950s and are used in surfactants and polymers, such as stain repellents for textiles, fire-fighting foams, grease-proof food contact paper, Teflon coatings, emulsifiers, and foaming agents. During 1972–2002, an estimated 96,000 tonnes of POSF (perfluorooctanesulfonyl fluoride) were produced worldwide (Prevedouros et al., 2006). Since then, given the extent of PFAS distribution in soils, water, and food webs, international authorities have taken measures to reduce their production. Under the US EPA's 2006 PFOA Stewardship Program, eight major fluorochemical companies committed to reducing the content of PFOA and related emissions and products by 95% (US EPA, 2006). Not all international manufacturers agreed to this, and production of some of these chemicals continues in China, India, and Russia, thus shifting the source of these pollutants from North American and European countries to developing Asian economies (AMAP, 2017) (Fig 5).

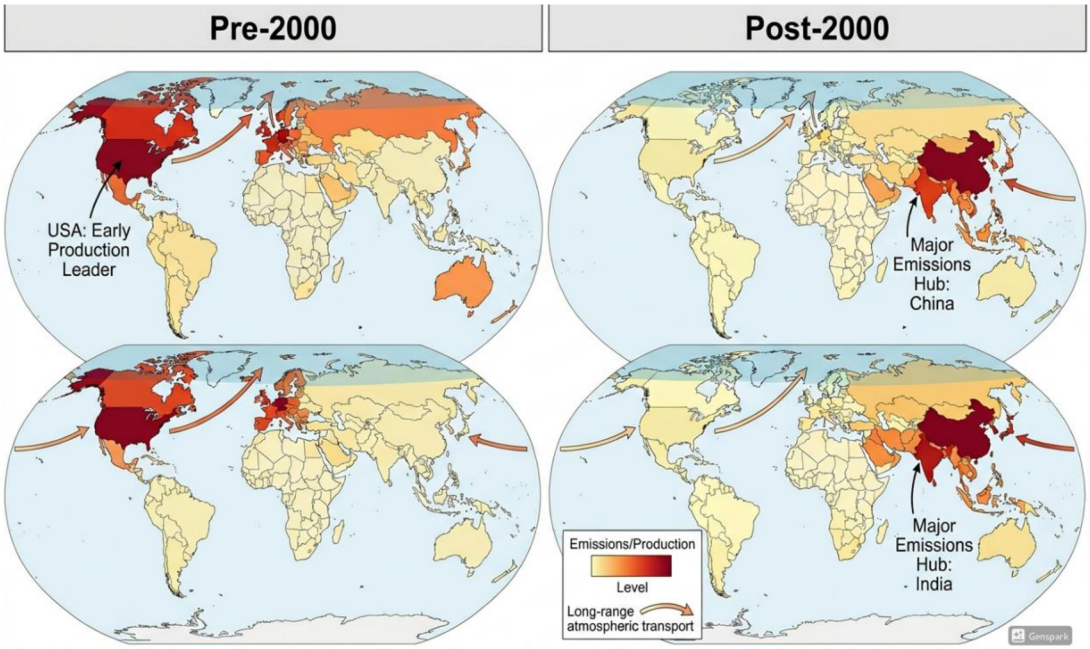

Fig 5: Global shift of PFAS emission sources from North America and Europe to Asia (Author's own elaboration based on sources cited in the text; visual layout assisted by GenSpark AI)

PFAS contamination is widespread in soil, water, and food chains due to decades of use since the 1940s. Soils near industries, upstream rivers, wastewater treatment plants (WWTPs), and landfills often show high concentrations of PFAS (AMAP, 2017). PFAS in drinking water are subject to regulations that vary by country, considering concentrations in source waters and groundwater. According to studies, approximately 45% of U.S. tap water contains at least one type of PFAS, though mitigation efforts have reduced levels, especially for PFOS, in the U.S. and Japan (AMAP, 2017). PFAS transfer through food occurs via bioaccumulation and follows trends similar to those in soil and water contamination. Dairy cattle with long-term exposure to PFAS-contaminated water or feed accumulate elevated concentrations of PFAS in milk, blood, and edible tissues, with higher levels observed in older animals due to the long biological half-lives of these compounds (AMAP, 2017). A similar pattern is observed in clams, freshwater and marine fish (e.g., Pacific cod far offshore Japan), and eggs from poultry raised in the European Union (EU), where PFAS contamination has been reported in eggs from free-range hens with access to contaminated soil (AMAP, 2017; EFSA, 2020). Blood biomonitoring worldwide has detected concentrations of PFAS in human bodies and has shown both rising and declining trends for legacy PFAS, suggesting the possibility of PFAS being eliminated from the human body through excretion, though elimination half-lives can exceed several years for long-chain PFAS (AMAP, 2017). In general, Food and drinking water are the major sources of PFAS entering the human body (AMAP, 2017).

3.4.2 PFAS Life Cycle Emissions

PFAS are discharged into the environment at various stages of their life cycle. First, emissions occur when products are manufactured at fluorochemical industrial sites. Second, PFAS are discharged when products are being used. Third, additional emissions occur during disposal, especially from wastewater treatment plants and landfills (AMAP, 2017). Studies examining global PFAS emissions have demonstrated that the most critical sources vary and can shift over time depending on the compound. For example, perfluorohexanesulfonic acid (PFHxS) emissions were thought to be primarily attributed to the atmospheric oxidation of sulfonamide- and sulfonamidoethanol-based precursor chemicals (Armitage et al., 2009), and perfluorodecanesulfonic acid (PFDS) emissions were more significantly related to, and strongly associated with, the product use and disposal (Wang et al., 2014). These differences in emission profiles reflect a key feature of PFAS environmental transport.

PFAS typically do not travel long distances in their final ionic form. Instead, volatile precursor compounds are transported through the atmosphere to remote places like the Arctic, where they undergo atmospheric oxidation to form stable PFCAs and PFSAs, resulting in widespread, diffuse contamination (Arulananthan et al., 2025; Roos et al., 2022). PFAS are present in air, rain, snow, and water. Some PFAS bioaccumulate and bio magnify in food webs, with their concentrations increasing at each successive trophic level (AMAP, 2017; Muir et al., 2025).

Human exposure pathways vary widely between regions. In contaminated areas near industrial sources, airports, and firefighting training sites, contamination of drinking water is usually a major concern. In remote locations, far from direct sources, people are usually exposed through their diet, particularly by consuming local wildlife that accumulate PFAS. This is especially important for Indigenous populations, whose culture and food security depend on these species (AMAP, 2017).

Elevated PFAS concentrations are consistently reported in soils near industrial facilities, airports, military bases, and firefighting training sites, where aqueous film-forming foams (AFFF) have been the primary source of local contamination (AMAP, 2017). These contaminated soils are a direct source of PFAS to adjacent groundwater and surface water bodies through leaching and runoff, resulting in bioaccumulation in fish and shellfish in affected water bodies (AMAP, 2017; Joerss et al., 2020).

3.4.3 Long-Range Transport to the Arctic

Long-range transport of PFAS to remote polar regions occurs via two primary pathways: oceanic circulation and atmospheric deposition of volatile precursors. While atmospheric deposition is critical for volatile PFAS precursors, PFCAs and PFSAs are predominantly transported as dissolved anions through ocean currents due to their low pKa values and high-water solubility, entering the Arctic primarily via the Fram Strait, the deep-water passage between Greenland and Svalbard, which serves as the main oceanographic gateway to the Arctic basin (Joerss et al., 2020). Secondary inputs occur through glacier and sea-ice melt (AMAP, 2017). Atmospheric transport is dominated by the oxidative degradation of volatile neutral precursors such as fluorotelomer alcohols (FTOHs) and perfluoroalkane sulfonamides (FASAs), which are oxidized in the atmosphere to form stable PFCAs and PFSAs that subsequently deposit onto the Arctic surface via wet and dry deposition (Arulananthan et al., 2025; Roos et al., 2022). Historical profiles of PFCAs from two ice cores collected on a glacier near the city of Longyearbyen (Svalbard) showed consistent patterns in the vertical profiles of PFCAs in both ice cores, dominated by PFBA (39%), followed by PFOA (17%) and (Perfluorononanoic acid) PFNA (11%). PFCAs were the major PFAS compounds in the ice cores (Kwok et al., 2013).

An investigation of seasonal variations in C4-C9 perfluoroalkyl acids in the surface snow of Svalbard revealed that concentrations are highly influenced by short-term solar radiation, indicating photochemical atmospheric degradation of volatile precursors as a key source of ionic PFAS deposition (Roos et al., 2022). In some cases, aerosol-bound transport also contributes to PFAS deposition in the Arctic, though to a lesser extent compared to precursor degradation (AMAP, 2017).

Recent Arctic air monitoring studies have reported high detection frequencies (>75%) for short-chain PFAS such as PFBA (perfluorobutanoic acid) and PFPeA

(perfluoropentanoic acid) (Arulananthan et al., 2025; Roos et al., 2022). In addition, concentrations of longer-chain legacy compounds, i.e., PFOA (C8 PFCA) and PFOS (C8 PFSA), have shown renewed increases in Arctic air after a period of stable decline since approximately 2019, possibly reflecting continued industrial use in regions without phase-out regulations (Arulananthan et al., 2025).

Joerss et al. (2020) detected 29 PFAS along transects from Europe to the Arctic and reported the first observation of hexafluoropropylene oxide dimer acid (HFPO-DA), i.e., a compound introduced as a PFOA replacement in industrial processes in Arctic seawater, providing direct evidence for long-range oceanic transport of next-generation PFAS substitutes. The investigation revealed that total PFAS levels were elevated in cold, low-salinity surface water leaving the Arctic (260 ± 20 pg/L), compared to North Atlantic water entering the Arctic (190 ± 10 pg/L), suggesting that the Arctic acts as a net source of some PFAS due to atmospheric deposition within the basin (Joerss et al., 2020). Mass balance estimates from this study indicated a net inflow of long-chain PFAS (those with ≥8 perfluorinated carbons, including PFOS and C9–C11 PFCAs) into the Arctic via Atlantic boundary currents, while shorter-chain PFAS (C4–C7 PFCAs) showed a net outflow via Polar Surface Water. This pattern is consistent with the preferential atmospheric deposition of short-chain PFAS within the Arctic and their subsequent release via meltwater, combined with greater retention of long-chain compounds in sea ice and snowpack (Joerss et al., 2020).

3.4.4 PFAS Accumulation in Different Environments

During winter, PFAS deposited from the atmosphere accumulate in snow and sea ice rather than volatilizing back to the atmosphere, owing to the low temperatures and high sorption capacity of the snowpack. Upon spring snowmelt and sea-ice thaw, these stored PFAS are released into local marine systems and terrestrial systems (via snowpack runoff), representing an important seasonal pulse of contamination to Arctic aquatic environments (AMAP, 2014). Kwok et al. (2013) studied PFAS concentrations in ice cores, surface snow, and water samples collected from glaciers and coastal areas distal from the city of Longyearbyen (Svalbard) to assess both local and background contamination levels. PFBA, PFOA, and PFNA were the predominant compounds found in ice-core samples. Elevated PFAS concentrations in snow and surface water near Longyearbyen were 2-3 times higher than at remote reference sites, suggesting that local anthropogenic activities, including airport operations, fuel handling, and wastewater discharge from the settlement, contribute to PFAS loading in addition to long-range atmospheric deposition. In surface snow samples, PFOA was the predominant PFAS detected, reflecting its relatively high abundance in atmospheric deposition. In contrast, glacial meltwater surface water samples were dominated by PFBA and perfluoropentanoate (PFPeA), consistent with the greater water solubility and mobility of these shorter-chain compounds, which are preferentially leached from the snowpack during melt (Fig 6).

A study of snow from the Devon Ice Cap in the Canadian Arctic (collected in 2008) recorded PFOA concentrations of 0.07-0.68 ng/L, PFNA of 0.03-1.42 ng/L, and (Perfluorodecanoic acid) PFDA of 0.0-0.23 ng/L (Young et al., 2007). These concentrations were of a similar order of magnitude to those reported by De Silva (2011) at Station Nord in northern Greenland (PFOA approximately 0.10-0.50 ng/L), suggesting that long-range atmospheric deposition is the dominant source of PFAS in both Canadian and Greenlandic High Arctic snowpacks rather than local sources.

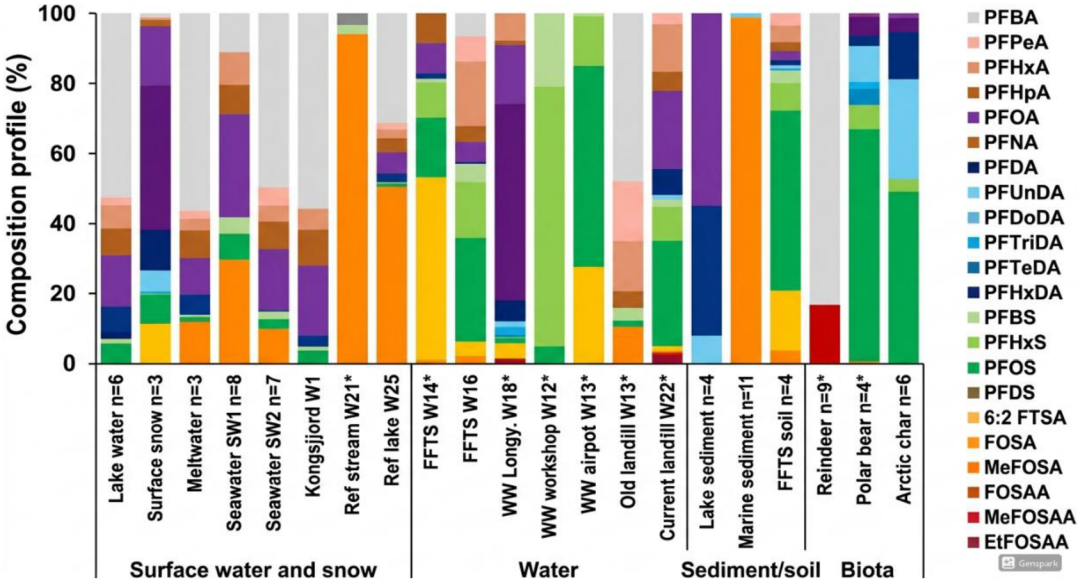

Fig 6: Concentration of different types of PFAS in Svalbard (Author's own visual, modification assisted by GenSpark AI)

An investigation of PFAS compounds in snow in northern Norway (Tromsø area) found that PFCAs (C4-C12) were the dominant group, with concentrations ranging from 0.294 to 5.206 ng/L (Roos et al., 2022). Only two of the PFSAs (PFBS and PFOS) were detected, with levels of PFBS varying from below the limit of detection to 0.178 ng/L. Concentrations of particle-bound PFAS were relatively low and typically below the detection limit. Levels of particle-associated PFBA were reported up to 0.383 ng/L, with the highest detection frequency in samples near the city of Tromsø. Deposition flux of PFCAs into the snowpack appeared to be affected by air temperature at the time of snowfall, with higher temperatures associated with greater fluxes. This may be due to enhanced scavenging of PFCAs from air by wet snow, and the possibility that snowflakes have a larger surface area in milder conditions, facilitating surface-mediated photochemical transformation of PFAS precursors (Roos et al., 2022). Hence, snowfall at mild temperatures results in significant levels of PFAS in the snowpack, where it accumulates over the winter and is released into the surrounding environment when the snow melts.

3.4.4.1 PFAS in Terrestrial Biota

Canada (Yukon and Nunavut)

Müller et al. (2011) measured PFAS in plants, moss, and lichen from the northern Yukon and western Nunavut near Bathurst Inlet, Canada. The lowest PFCA concentrations were detected in sedge (*Carex aquatilis*) and cottongrass (*Eriophorum vaginatum*) in the northern Yukon (0.01–0.02 ng/g ww), while cottongrass at Bathurst Inlet showed elevated concentrations, likely reflecting proximity to industrial sources. PFAS patterns differed significantly between vascular plants and lichen, with odd-carbon-chain PFCAs predominating in caribou (*Rangifer tarandus*), wolf (*Canis lupus*), grasses, and moss, while PFOA predominated in willows and grasses (Müller et al., 2011). This study also assessed the biomagnification of PFAS from vegetation to caribou and wolf. Biomagnification factors were tissue-specific and highest for C9-C11 PFCAs (BMF 2.2-2.9) and PFOS (BMF 2.3-2.6), values that are lower than those reported for marine food webs. Wolf liver contained the highest ΣPFAS concentrations among terrestrial species, as expected for an apex predator, followed by caribou liver. ΣPFCAs/PFOS ratios, which serve as an indicative measure of PFAS profile composition, reflecting the relative predominance of PFCAs over PFOS, exceeded 10 in vegetation and ranged from 5 to 10 in mammals, while muscle and kidney concentrations were 10-20 times lower compared to liver (Müller et al., 2011).

Svalbard and Scandinavia

In Svalbard reindeer (*Rangifer tarandus platyrhynchus*), muscle tissue was dominated by the long-chain PFCAs, i.e., perfluoro dodecanoic acid (PFDoDA; C12) and perfluoro tridecanoic acid (PFTrDA; C13), while liver contained predominantly PFNA (C9) and PFTrDA, closely followed by PFOS and PFHxS. Moreover, long-chain PFCAs were also detected in fat tissue. In contrast, PFAS profiles in southern Greenland reindeer liver were dominated by PFOS (1.42 ng/g ww), followed by PFNA (0.84 ng/g ww) and perfluoroundecanoic acid (PFUnDA; 0.45 ng/g ww). Swedish reindeer (*Rangifer tarandus*) muscle samples collected between 1987 and 2006 contained detectable but unquantifiable levels of perfluorooctanesulfonamide (PFOSA), PFOS, and PFOA, reflecting the historical presence of legacy PFAS at low concentrations in Scandinavian wildlife. Norwegian moose (*Alces alces*) liver was dominated by PFOS, followed by PFNA, PFUnDA, and PFDA (AMAP, 2017).

3.4.4.2 PFAS in Freshwaters

PFAS concentrations in remote Arctic lakes (such as Amituk, Char, Meretta, and Resolute lakes on Cornwallis Island) are low and similar to atmospheric deposition patterns observed in North American precipitation and glacier ice, with mean PFOA concentrations of approximately 0.20–0.27 ng/L (De Silva et al., 2011). Resolute and Meretta Lakes, located near an airport, show elevated concentrations of PFOS and

PFHxS attributable to aqueous film-forming foam (AFFF) use, alongside fluorotelomer sulfonates (FTS) and perfluoroethylcyclohexanesulphonate (PFECHS), two PFAS compounds used as aircraft hydraulic fluid additives (AMAP, 2017; De Silva et al., 2011). In Svalbard, rivers near the city of Longyearbyen show elevated concentrations of PFBA and PFPeA, with values approximately 2 to 3 times higher downstream of the settlement, indicating the influence of local sources (Kwok et al.,2013). In general, in freshwaters across the Arctic, PFAS contamination is widespread, with long-chain PFCAs and especially C9-C12 compounds (PFNA, PFDA, PFUnDA, PFDoDA), generally found to be the dominant forms in fish tissue (AMAP, 2017). Regional differences are notable: fish in Norway and Greenland contained higher concentrations of long-chain PFCAs, while samples from Canada showed lower overall PFAS concentrations and a less pronounced dominance of longer-chain homologues, potentially reflecting differences in proximity to emission sources and oceanic transport routes (AMAP,2017).

3.5 Arctic as Sink and Source

The primary question in Arctic PFAS studies is whether the Arctic acts primarily as a sink (accumulating PFAS from global releases) or a source (releasing stored PFAS back into the global environment). The Arctic can serve both functions (Fig 7), depending on the specific PFAS compound and environmental conditions (AMAP, 2017; Dunn et al.,2024). The Arctic is predominantly known as a sink for many PFAS compounds, particularly short-chain PFCAs formed from atmospheric degradation of volatile precursors, as has been previously mentioned. Analysis of ice cores affected by continuous precipitation and accumulation clearly indicates increasing PFAS concentrations over time. Low temperatures promote cold condensation and deposition of semi-volatile compounds, and large areas of ice increase sorption capacity (AMAP, 2017). The Arctic can also function as a secondary source of PFAS under conditions of rising temperatures, when melting glaciers, thawing permafrost, and deteriorating sea ice release historically accumulated PFAS back into aquatic systems and the atmosphere (Vidal et al., 2019). Joerss et al. (2020) determined that total PFAS concentrations were elevated in cold, low-salinity surface water leaving the Arctic compared to incoming North Atlantic water. Dunn et al. (2024) estimated that total PFAS export from the Arctic via ocean currents slightly exceeded import, and interpreted this net outflow as evidence that substantial atmospheric PFAS deposition occurs within the Arctic basin, contributing material that is subsequently exported to the North Atlantic via surface currents. In the Lake Hazen watershed (Canadian High Arctic), Vidal et al. (2019) calculated total PFAS inputs of 2.04 kg (1.6 kg from glacial rivers, 0.44 kg from snowmelt) and output of 0.64 kg, representing an annual net accumulation of 1.4 kg. This means that a large proportion of PFAS remains stored in the watershed, but at the same time, a considerable amount is also transported downstream. Climate change is expected to shift the Arctic increasingly toward functioning as a secondary source rather than a sink. PFAS stored in cryospheric reservoirs will become mobilized and released into aquatic systems as

temperatures increase and snow and ice continue to melt. Ahrens et al. (2011) were the first to identify melting snow and ice as diffuse secondary PFAS sources that could increase with climate change. This indicates that contamination does not come from a single point source but from spatially distributed releases. Even if global PFAS emissions decrease, PFAS stored in these reservoirs can continue to act as a source, contributing to sustained or increased concentrations in Arctic wildlife and aquatic organisms (Ahrens et al., 2011; AMAP, 2017).

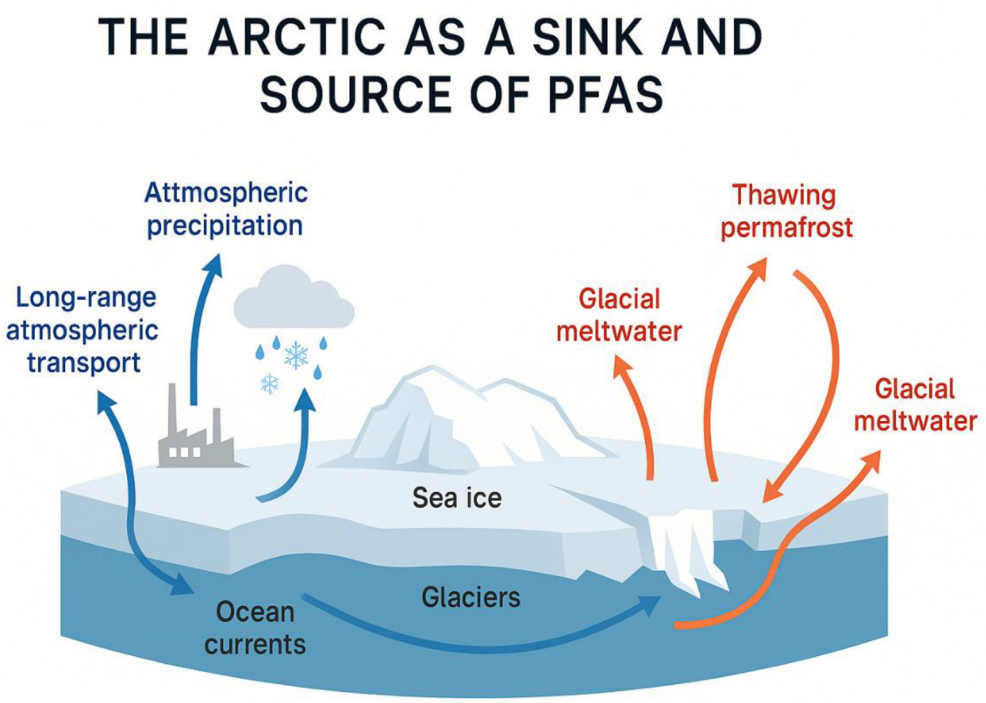

Fig 7: Arctic as a sink and source of PFAs (Author's own elaboration based on sources cited in the text; visual layout assisted by Microsoft Co-pilot).

3.6 Methods for Sampling Soil and Water Contaminated with PFAS

To analyze PFAS concentrations, traditional grab sampling methods have been widely used. However, for long-term tracking, transport, preservation, and storage, these methods are not ideal. In such cases, passive sampling methods are considered a good choice. They could be highly effective for transporting and preserving samples, providing better insights into the samples and additional information on the bioavailability of chemicals (Yang et al., 2022). Several types of water passive sampling devices have been used, such as the diffusive gradient in thin film technique (DGT), polar organic chemical integrative sampler (POCIS), semi-permeable membrane devices (SPMDs), and membrane-enclosed sorptive coating (MESCO). It is easy to use such passive sampling devices in two different ways during field exposure: the kinetic linear uptake mode, in which analyte accumulation in the sorbent increases linearly with time, and is proportional to the time-weighted average

concentration in the surrounding water, and the equilibrium mode, in which the analyte concentration in the sampler reflects equilibrium partitioning between the sampler and the surrounding medium Vrana et al. (2005).

Concerning the concentrations, PFAS occur in environmental matrices across a wide concentration range, from sub-ng/L (parts per trillion) levels in remote Arctic waters to µg/L concentrations near point sources such as AFFF-impacted sites and are typically present with a complex mixture of other organic compounds (Arulananthan et al., 2025; AMAP, 2017). While concentrations in pristine Arctic environments are low, they are not toxicologically insignificant, as PFAS bioaccumulate and bio magnify in food webs, resulting in tissue concentrations in top predators that may exceed health-based thresholds (AMAP, 2017). At the relatively low dissolved PFAS concentrations, passive samplers offer a distinct analytical advantage over conventional grab sampling, as they accumulate analytes over extended deployment periods to levels above instrumental detection limits and provide TWA concentrations that are more representative of long-term exposure conditions (Hale et al., 2021).

3.6.1 Grab Sampling

Grab sampling means collecting water samples from a specific location at a specific time. This is the most common and officially recommended method for measuring PFAS levels in water. It captures the PFAS loading at that moment, so it is best used when the main goal is analyzing contaminants at a specific time, identifying sudden contamination events, or checking if PFAS is present at a site. In practice, grab samples for PFAS analyses are collected using special, lab-supplied high-density polyethylene (HDPE) or polypropylene (PP) containers. These are filled directly from the water source, ensuring the sample is not shaken or agitated. For drinking water, samples are usually taken from taps in the distribution system after flushing. For surface water, samples are collected at a set depth, avoiding the surface foam where PFAS can accumulate due to their surfactant properties (California SWRCB, 2020).

Grab sampling is popular because it is simple, low-cost, and keeps the sample intact, avoiding the problems that come with storing samples in the field for a long time. However, its main drawback is that a single grab sample might miss short-term contamination events, daily changes in concentration, or the average exposure over time, which is most important for risk assessment (Kaltenberg et al., 2022). For groundwater grab sampling, it is important to use dedicated or well-purged equipment. Low-flow purging methods, which take water from the screened part of the well at a steady rate, are preferred for PFAS testing. These methods maintain water quality indicators, such as pH, specific conductance, dissolved oxygen, oxidation-reduction potential, and turbidity, at stable levels by minimizing hydraulic stress at the well-aquifer interface, which, if excessive, can cause re-suspension of particulates, degassing of volatile analytes, and physicochemical alteration of the sample (US EPA, 2017). Guidance from several US states and the US EPA recommends low-flow sampling for PFAS groundwater testing, especially when samples have high turbidity that could affect results (NJ DEP, 2021).

3.6.2 Passive Sampling

Passive sampling is a very different approach from grab or composite sampling methods (where multiple grab samples are pooled together to represent an average over time or space). Instead of extracting a single water sample from the environment, samplers are left in the water for days or even weeks. During this time, chemicals from the water gradually move into a special material inside the sampler, which captures them for later analysis. Once the sample is collected, the chemical buildup can be measured and, using the device's sampling rate (called Rs), the average amount of that chemical in the water over the entire time the device was in place can be determined. This method smooths out any spikes or dips in concentration that might happen from hour to hour or day to day (Huckins et al., 2006). This "time-averaged" feature is a major advantage of passive sampling, since it gives a much better picture of long-term exposure than a single grab sample ever could. Several types of passive samplers have been tested or are already being used to monitor PFAS in water. One of the first was the polar organic chemical integrative sampler (POCIS). This device is used to detect ionic PFAS in rivers, lakes, and wastewater. It works best when chemical concentrations are low, such as in uncontaminated or minimally impacted surface waters. Another alternative to POCIS samplers is the DGT (Diffusive gradients in thin films) samplers. Unlike many other passive samplers, which require a lot of trial-and-error to determine how much they collect, DGT uses a simple, well-understood method. It relies on natural diffusion, the way substances move from high to low concentration, which means you can directly calculate how much of a chemical is present in the water without having to calibrate the device for every new location (Zhang & Davison, 1995). Other example is the Sentinel passive sampler, which is sold commercially and uses a specially modified resin called Osorb. This material includes added amine groups (to facilitate ion exchange) and copper ions (to enhance its ability to bind PFAS). This sampler has demonstrated its ability to collect various PFAS from groundwater, rivers, and other water bodies.

3.6.2.1 POCIS

The POCIS device was developed by the researchers at the USGS Columbia Environmental Research Centre in the late 1990s, and Alvarez et al. (2004) described its foundational design. They created it to fill a monitoring gap left by semipermeable membrane devices (SPMDs), which work well for hydrophobic compounds (log K_{ow} 4-8) but are ineffective for sampling polar, hydrophilic organic contaminants (HpOCs) with log $K_{ow} < 3$ (Alvarez et al., 2007). The first field use of POCIS was reported in 2004, mainly to detect pharmaceuticals and pesticides in wastewater treatment plant effluents (Alvarez et al., 2007). Alvarez and colleagues first used POCIS for PFAS monitoring in wastewater in 2007 (USGS, 2024), and further improvements to PFAS uptake kinetics were published from 2010 onwards (Kaserzon et al., 2012). Researchers have used POCIS samplers in rivers downstream from paper mills and in wastewater treatment plants. They found that POCIS results generally match well with traditional grab samples, although the exact numbers can vary depending on the

material used in the sampler and the specific water chemistry at each site (Langberg et al., 2021). Researchers have also observed that POCIS samplers filled with hydrophilic-lipophilic balance (HLB) material typically collect about 2.3 times more PFAS than those filled with WAX (weak anion exchange) material. This means it is important to calibrate each device type for accurate results. One major challenge with passive PFAS sampling is that PFAS can exist in many forms. Materials that work well for capturing non-polar chemicals usually do not work for the small, anionic, short-chained PFAS that have increasingly become the focus of regulatory concern as longer-chain compounds are phased out and replaced by shorter-chain alternatives (Gobelius et al., 2019).

Components of POCIS Sampler

A standard POCIS device comprises a granular solid sorbent receiving phase enclosed between two microporous polyethersulfone (PES) membranes (pore size 0.1 µm, thickness 100 - 200 µm). These membranes are secured by two stainless steel rings, providing a sampling surface area of approximately 41 - 46 cm^2 (Alvarez et al., 2007; Gardiner et al., 2022). The typical surface area-to-sorbent mass ratio ranges from 180 to 227 $cm^2\ g^{-1}$ (Gobelius et al., 2019; Alvarez et al., 2007). During deployment, POCIS disks are mounted on a support rod, usually made of stainless steel or PVC, to shield the sampler from physical debris and biofouling. Two commercial configurations are usually available: a "generic" configuration with 3 sorbent materials for pesticides and wastewater analyses, and a second configuration for pharmaceuticals with a single sorbent (Fig 8) (Alvarez et al., 2004). Multiple disks may be combined to increase the accumulated analyte mass, and narrow-format variants have been developed for use in groundwater monitoring wells.

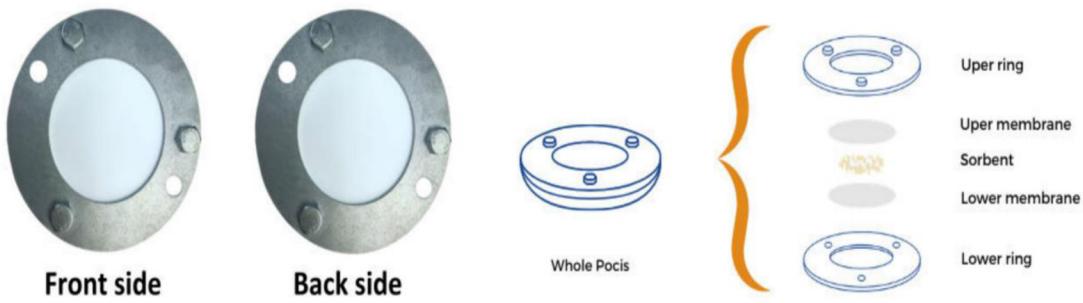

Fig 8: Components of POCIS sampler (AFFINISEP, ©2026).

Accurate calibration of sampling rates is essential for the quantitative application of POCIS in estimating PFAS time-weighted average (TWA) concentrations. Two primary calibration methods are recognized: laboratory calibration, which employs static renewal or flow-through systems, and in situ field calibration through co-deployment with active sampling (Harman et al., 2012). Laboratory calibration under controlled conditions is the most widely used approach. However, sampling rate (Rs) values determined in the laboratory often differ significantly from those measured in situ, especially in low-flow environments such as groundwater. Studies using

groundwater pilot systems have reported Rs values that are 1-14 times lower than those observed under stirred laboratory conditions, due to the substantially reduced water flow velocities in subsurface environments (Kaserzon et al., 2019). The pronounced dependence of Rs on flow velocity highlights the need for environment-specific calibration for accurate PFAS monitoring (Gardiner et al., 2022; Duan et al., 2020).

3.6.2.2 DGT

The DGT device was invented in the early 1990s by Davison and Zhang at Lancaster University. It was originally designed to measure low concentrations of metals in freshwater, focusing on how those metals exist in different chemical forms (Davison & Zhang, 1994). The idea behind DGT is quite simple: it combines a thin layer that lets chemicals slowly pass through (the diffusion layer) and a layer that captures and holds them (the binding phase), all packed into a small, easy-to-use device.

Since its invention, DGT has proven to be a highly adaptable and flexible tool. Scientists have used it to measure a wide variety of substances in different environments and not just trace metals and metalloids like Cd, Pb, Cu, Zn, and As, but also nutrients like phosphate, radioactive elements, and organic pollutants such as herbicides, pharmaceuticals, and polycyclic aromatic hydrocarbons (Zhang et al., 1998; Gao et al., 2016). More recently, DGT has been adapted for PFAS monitoring by developing specialized binding phases and membrane materials tailored to the chemical properties of ionic PFAS. Early development of DGT for PFAS monitoring explored mixed-mode sorbents such as Oasis WAX and Strata-X-AW, which combine reversed-phase (hydrophobic) and anion-exchange functionality to retain both long- and short-chain anionic PFCAs and PFSAs (Zhou et al., 2024). The current standard DGT configuration in this study for perfluorinated compounds (LSNW-AP, DGT Research Ltd) employs a WAX binding gel, a 0.8 mm agarose diffusive gel, and a polyethersulfone (PES) filter membrane (0.14 mm), applicable across freshwater to seawater matrices, the agarose gel minimizing non-specific PFAS retention in the diffusion layer, and the PES membrane reducing non-specific sorption given the surfactant properties of these compounds (DGT Research, 2023).

Principle of DGT

Diffusive Gradients in Thin-films (DGT) utilizes molecular diffusion to accumulate analytes from solution onto a binding agent or gel at a rate proportional to the analyte concentration in the solution. The device establishes a defined concentration gradient across a diffusive gel layer, and the analyte flux through this layer is described by Fick's first law of diffusion:

$$J = -D\,(dC/dx)$$

In this equation, J represents the flux (mol $cm^{-2}s^{-1}$), D is the diffusion coefficient of the analyte in the gel ($cm^2\ s^{-1}$), and dC/dx denotes the concentration gradient across the diffusion layer (Davison & Zhang, 1994). Under steady-state conditions, the

binding resin removes the analyte at its surface, and the concentration at the outer face of the diffusive gel equals that of the bulk solution. This results in a linear concentration gradient. The mass of analyte accumulated (M) over a deployment time (t) is given by:

$$M = D \times A \times C \times t / \Delta g$$

where A denotes the exposed area of the device, C (ng mL^{-1}) is the time-averaged concentration of labile analyte in the bulk solution, and Δg (cm) is the thickness of the diffusive gel layer. Importantly, this method quantifies only the kinetically labile fraction of the analyte, defined as species capable of dissociating from natural ligands and diffusing through the gel within the experimental timescale. As a result, DGT is inherently selective for the most bioavailable and ecotoxicologically relevant fraction (Davison & Zhang, 1994).

DGT Components

The conventional diffusive gradients in thin films (DGT) device consists of a plastic case, generally made from polycarbonate or Delrin, which includes a piston and a cap with a circular opening. The main components of this assembly are (1) a filter membrane, (2) a diffusive gel layer, and (3) a binding phase gel or resin disc (Fig. 9) (Zhang & Davison, 1995). The current standard DGT configuration in this study for perfluorinated compounds (LSNW-AP, DGT Research Ltd) employs a WAX binding gel, a 0.8 mm agarose diffusive gel, and a polyethersulfone (PES) filter membrane (0.14 mm), applicable across freshwater to seawater matrices, the agarose gel minimizing non-specific PFAS retention in the diffusion layer, and the PES membrane reducing non-specific sorption given the surfactant properties of these compounds (DGT Research, 2023). The binding phase quantitatively retains the analyte of interest. The housing secures the entire assembly and is engineered to prevent solution from bypassing the gel layers (Zhang & Davison, 1995).

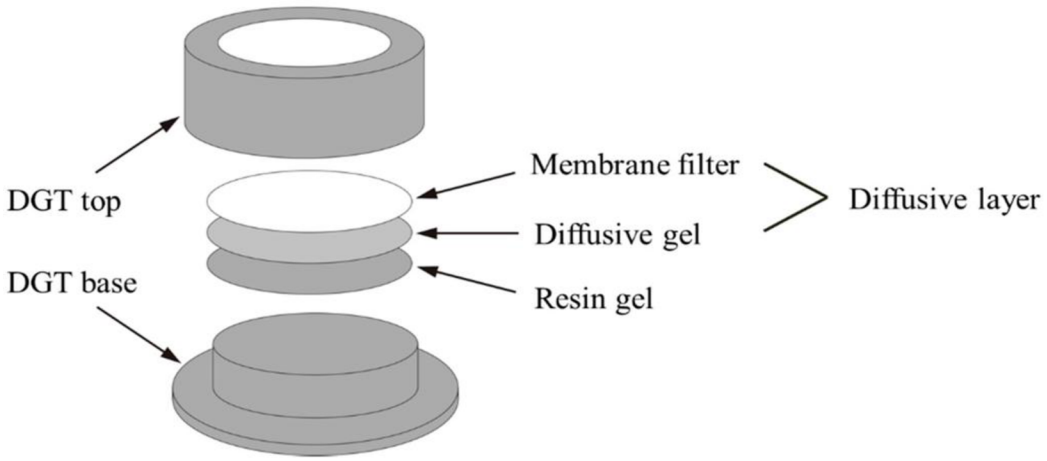

Fig 9: Components of a DGT sampler (Yao et al, 2016)

3.7 PFAS Analytical Methods

Conventionally, PFAS are usually analyzed using liquid chromatography coupled with mass spectrometry, especially LC-MS/MS or gas chromatography. Currently approved U.S. EPA methods typically involve solid-phase extraction (SPE) to concentrate PFAS from water samples followed by LC-MS/MS analysis. Identification is based on several factors, such as retention time in the chromatography system and the type of anion and cation, compared with known reference standards. Chromatography better separates chemicals in a mixture, making detection easier. The majority of EPA-approved analytical methods for PFAS determination are based on LC-MS/MS (US EPA, 2021). But for some neutral and volatile PFAS, gas chromatography (GC-MS) is preferred. However, POCIS and DGT passive samplers inherently concentrate target analytes within the sorbent or binding phase during deployment according to manufacturer's recommendations, which allows them to be analyzed directly. Over the years, the use of the TOP (total oxidizable precursors) assay has increased markedly. Moreover, several studies have reported a growing use of high-resolution accurate-mass spectrometry (HRMS) together with improved TOP methodologies (Nahar et al., 2023).

4. METHODOLOGY

4.1 Description of The Study Area

The Svalbard archipelago is a Norwegian High Arctic territory situated between 74° and 81° North latitude and 10° to 35° East longitude, positioned approximately midway between mainland Norway and the North Pole (Liestøl, 1993). Covering a total land area of approximately 62,248 km², the archipelago comprises four main islands, Spitsbergen (the largest at ~39,000 km² and the only permanently inhabited island), Nordaustlandet, Edgeøya, and Barentsøya, together with numerous smaller islets and skerries (Fig 10) (Liestøl, 1993). The administrative capital, Longyearbyen, is located on the western coast of Spitsbergen along the shores of Adventfjorden (a branch of Isfjorden) and serves as the principal settlement and logistical hub for scientific activity in the archipelago (Førland et al., 2011).

Fig 10: Map of the Svalbard Archipelago (World Atlas).

Glaciers and ice caps dominate the physical landscape of Svalbard, covering approximately 59% of the total land area and encompassing more than 2,100 individual glaciers with a combined area of ~34,000 km² (Liestøl, 1993; Spolaor et al., 2024). These glaciers and ice caps represent approximately 6% of the global glacier area outside the Greenland and Antarctic ice sheets, and contain sufficient ice volume

to raise global mean sea level by an estimated 1.7 ± 0.5 cm if fully melted (Spolaor et al., 2024). The entire archipelago lies within the zone of continuous permafrost, with the thickness ranging from less than 100 m near the coasts to more than 500 m in the interior highlands (Humlum et al., 2003). Permafrost exerts a fundamental control on hydrology and solute transport in the region, limiting vertical infiltration and concentrating contaminant fluxes in surface and near-surface flow paths (Humlum et al., 2003; Grünberg et al., 2024). Active layer depths near Longyearbyen have been increasing in recent decades; at the Janssonhaugen monitoring station, active layer depth increased from 1.6 m (1999) to nearly 2 m (2016), and at a coastal Adventdalen site, deepening proceeded at a rate of 0.7 cm yr^{-1} between 2000 and 2018 (Grünberg et al., 2024).

4.2 Sampling Sites

Two sampling sites were established in the vicinity of Longyearbyen for this study (Fig 11). Site A was located adjacent to Svalbard Airport, on the coastal plain associated with the airport's firefighting training infrastructure. Given the well-documented link between airport AFFF use and elevated PFAS concentrations in surrounding soils and sediments (Skaar et al., 2019), this site was selected as the primary location for sediment collection. Site W was located in Adventfjorden near Longyearbyen Harbour, representing an Arctic fjord environment subject to multiple overlapping PFAS inputs from wastewater, urban runoff, airport drainage, and glacial meltwater (Ahrens et al., 2023). At both sites, passive water samplers (DGT and POCIS) were deployed to capture time-integrated, bioavailability-relevant PFAS concentrations in the water column.

Sediment samples were collected only from a location near the airport in Spitsbergen, i.e. from a location with an expected higher content of PFAS considering previous activities and the currently ongoing remediation after the use of AFFF for firefighting training.

4.3 Sample Collection

The sediment samples were collected only from a location close to the Svalbard airport, i.e., one with expected higher PFAS content given previous activities and the ongoing remediation after the use of this area for firefighting training using AFFF. The water samples were collected from both sites, i.e., a small lake near the Svalbard airport (A) and the fjord close to the wastewater discharge (W). Two types of passive samplers were used, DGT (LSNW-AP), purchased from DGT Research Limited, Lancaster, UK, and POCIS (AttractSPE POCIS-PFAS) from Affinisep. The samplers were deployed strictly following the manufacturer's instructions. Both of the passive samplers were deployed in water for 30-35 days for A and W, respectively.

Fig 11: Sampling sites A and W from where the water, sediment, and passive samplers were taken (Google Earth).

4.4 Preliminary testing of DGT samplers in a laboratory environment

A preliminary test was conducted in laboratory conditions to evaluate the extraction efficiency of DGT samplers in both freshwater and seawater before field use. The DGT samplers were obtained from DGT® Research (Lancaster, UK). They consist of a polyethersulfone (PES) filter membrane (0.14 mm thick), a permeable diffusive layer of 0.8 mm agarose diffusive gel, and a weak anion exchanger (WAX) binding gel layer, assembled together in a plastic holder. Deionized water was used as a freshwater equivalent. To prepare seawater in the laboratory, a concentrate of seawater "Absolute Ocean" (8.33-fold concentrated) was purchased from ATI (Germany). This concentrate is composed of laboratory-tested pure salts and is beneficial for replicating the exact composition of seawater throughout the experiment. The concentrate was diluted with deionized water according to the manufacturer's instructions. All other chemicals were of analytical grade.

An HDPE container was filled with 2 liters of either freshwater or seawater. The water was then spiked at 0.5 ppb with one of the four following tested PFAS analytes: PFOA, PFOS, PFBA, or PFBS. Batch tests were performed in triplicate. A procedural blank was run in each sample batch. A water volume of 500 µL was sampled several times during the test to check the PFAS content in the water, as PFAS are known to adsorb onto the walls of the container (Zenobio et al. 2022). First time before the DGT sampler was added, second time after its removal, and the third time after one hour at the ultrasound cleaner. Each water sampling was performed in duplicate.

To allow the DGT samplers to float freely in the water, they were attached to a polyester thread, which was attached to the neck of the container, and then inserted into the containers. The containers were shaken at 60 rpm on an orbital shaker for 24 hours at room temperature. After that, the DGT samplers were removed from the containers and disassembled into two parts, which were left fully immersed in MeOH containing 0.5% NH_3 for at least 24 hours. First part, the binding gel, was eluted inside capped 15 mL PP centrifuge tubes, which held 10 mL of the elution solution. The second part, the rest of the DGT sampler (filter, diffusive gel, cap, base) including the thread, was eluted inside a 250 mL glass beaker covered with parafilm, holding 50-60 mL of the elution solution. After 24 hours, the containers were opened, the binding gel as well as the DGT sampler were removed, and the content of the glass beaker was transferred into a 50 mL PP centrifuge tube. The eluents were left to evaporate to a volume of 500-1000 µL in the fume hood. Subsequently, the samples were transferred into 2 mL autosampler vials, and the tubes were rinsed with 500 µL of MeOH, which was then added to the vials. For further calculations, the vials were weighed empty and then after adding the samples. The samples were then passed for using liquid chromatography tandem mass spectrometry (LC-MS/MS). The principle of concentration calculation is presented in the following subchapter, and follows the manufacturer´s recommendations. To calculate the diffusion coefficient, an accurately measured temperature of 20°C was further used.

For a possible comparison of the performance of DGT samplers, recovery was subsequently calculated, i.e., for a direct comparison of the concentration in solution and the amount captured in the gel after conversion to the specified time and temperature. The recoveries are calculated using the following equation,

$$Recovery(\%) = \frac{c_{expected}}{c_{measured}} * 100$$

Where c (expected) is the concentration determined at a given stage (T0, T1, T2, or in the DGT gel; different time intervals are explained later in the text) and c (measured) is the theoretical post-spike concentration (0.5 µg/L). Recoveries were calculated separately for each replicate and then summarized as mean ± standard deviation. Recoveries in the range of 60-140% were considered acceptable for method performance and for use in quantitative interpretation. Values outside this range were treated as indicative of significant losses, contamination, matrix effects, or other artefacts and were therefore interpreted with caution or excluded from further quantitative evaluation.

Precision of the analytical results was evaluated using the relative standard deviation (RSD), which expresses the spread of replicate measurements relative to their mean and is reported as a percentage. RSD was calculated as:

$$RSD(\%) = \frac{SD}{\underline{x}} * 100$$

Where SD is the standard deviation and x is the mean.

Low RSD values indicate that measurements are tightly clustered around the mean (high precision), while high RSD values indicate poor repeatability and greater uncertainty.

4.5 PASSIVE SAMPLERS FROM THE FIELD

4.5.1 DGT PFAS Extraction

The DGT devices were deployed in the field following the instructions from the manufacturer. Following retrieval, DGT devices were thoroughly rinsed with ultrapure water and transported to the laboratory in clean plastic bags (Fig 12). Five DGT replicates were deployed per sampling site.

Fig 12: DGT devices labelled and assembled prior deployment.

The device cap was removed by twisting with a screwdriver, and the filter membrane and diffusive gel were peeled off to expose the binding layer. The WAX binding gel was fully immersed in 10 mL methanol (MeOH) containing 0.5% NH_3 and left for at least 24 hours at room temperature to elute the accumulated analytes. After removal of the binding gel, the eluate was evaporated to a volume of 500-1000 µL in the fume hood and transferred into 2 mL autosampler vials. For further calculations, the vials were also weighed empty and then after adding the samples. Compared to the manufacturer´s manual, the filtration step through a 0.22 µm syringe filter was omitted. Subsequently, the samples were analyzed immediately or stored in the fridge until analysis. Quantitative analysis of the reconstituted extracts was performed using liquid chromatography tandem mass spectrometry (LC-MS/MS).

Moreover, field blanks (DGT devices transported to the field site, briefly exposed during deployment preparation but not deployed, then returned for treatment and analysis) were included at a minimum of one field blank per test series.

The time-weighted average concentration of each analyte in water, was calculated using the standard DGT equation:

$$cDGT = \frac{M\Delta g}{DApt}$$

cDGT (ng/mL) is the time averaged concentration of analyte in the deployment medium measured by DGT. M (ng) is the mass of an analyte accumulated in the binding layer. Δg (0.094 cm) is the total thickness of the materials in the diffusion layer (diffusive gel and filter membrane).

D (cm^2 s^{-1}) is the diffusion coefficient of analyte in the material diffusion layer at the temperature during deployment. Standard values of D are available for 25°, values for other temperatures must be converted according to the manufacturer´s recommendation. Ap (3.14 cm^2) is the physical area of the exposed filter membrane or the window of the DGT device, t (s) is the deployment time.

The fraction of analyte that is successfully recovered from the DGT gel during extraction is elution efficiency and the values are given in the DGT manufacturer's website (Table 1).

Tab 1: The compounds that can be measured with LSNW-AP device and their elution factor, fe, values (DGT research).

Compound	**D ($\times 10^{-6}$ cm^2/s, 25 °C)**	**f_e**
6:2 FTSA	4.96	1.00
GenX	5.00	1.00
PFBA	6.46	1.00
PFBS	6.22	1.00
PFDA	3.46	1.00
PFHpA	5.87	0.95
PFHpS	5.62	0.95
PFHxA	5.33	1.00
PFHxS	5.04	0.95
PFNA	4.12	1.00
PFOA	4.75	1.00
PFOS	4.55	0.95
PFPeA	6.06	1.00
PFPeS	5.87	0.95

The mass, M, of analyte in the binding layer, is calculated from the measured concentration of analyte, c_e (ng/mL), in the elution solution, of volume V_{re} (m/L), f_e is the elution efficiency, remembering to take into account any subsequent dilution or pre-concentration:

$$M = \frac{c_e\, Vre}{f_e}$$

The temperature of the samples was measured onsite, at the time of collection, pH and conductivity were measured later in the laboratory.

Tab 2: Physical parameters of water samples

Location	**Temperature (°C)**	**pH**	**Conductivity (µS/cm)**
Airport	8	7.05	672
Wastewater	6.5	7.33	7160

The two sampling sites differed clearly in all three measured physical parameters. The airport site had a temperature of 8°C, a pH of 7.05, and a conductivity of 672 µS/cm. The wastewater site had a slightly lower temperature of 6.5°C, a higher pH of 7.33, and a significantly higher conductivity of 7160 µS/cm. Both sites recorded near-neutral pH values, within the range of 7.05–7.33. The most striking difference between the two sites was conductivity, with the wastewater site showing a value approximately 10-fold higher than the airport site.

The physical parameters measured at the two sites reflect distinct water types. The airport site conductivity of 672 µS/cm is within the range expected for surface freshwater or mildly impacted runoff, while the wastewater site conductivity of 7160 µS/cm falls in the higher range associated with a significantly higher dissolved ion load. The airport site, located in the fjord near Longyearbyen, represents brackish surface water influenced by inflowing glacial rivers, whereas the wastewater site reflects a more saline and ion-rich water type. (Fondriest Environmental, 2014). Both pH values (7.05 and 7.33) are within the near-neutral range, which is relevant for passive sampler performance. Zhang et al. (2021) demonstrated that WAX-DGT binding efficiency remains stable across pH 3-9 and ionic strength 1-500 mM, suggesting that the pH conditions at both sites are unlikely to have negatively affected DGT performance.

4.5.2 POCIS Extraction

Two POCIS samplers were tested, namely POCIS-PFAS and POCIS-HLB. AttractSPE POCIS-PFAS samplers (Affinisep, France) were used for passive water sampling of perfluorinated compounds. Each sampler contains approximately 235 mg of sorbent enclosed between two membranes, with an inner diameter of 55 mm, external diameter of 90 mm, and a specific surface area of approximately 200 cm^2/g. Each POCIS is single-use. Samplers were stored in the freezer prior to deployment. Three POCIS replicates were deployed per sampling site.

Following retrieval from the field, the outer membranes of each POCIS were rinsed with mineral water to remove surface contamination. Empty 6 mL SPE cartridges fitted with polyethylene (PE) frits were weighed prior to use to allow determination of dry sorbent mass. The POCIS was then opened and the sorbent powder was carefully transferred from the membranes into the pre-weighed SPE cartridge (Fig 13).

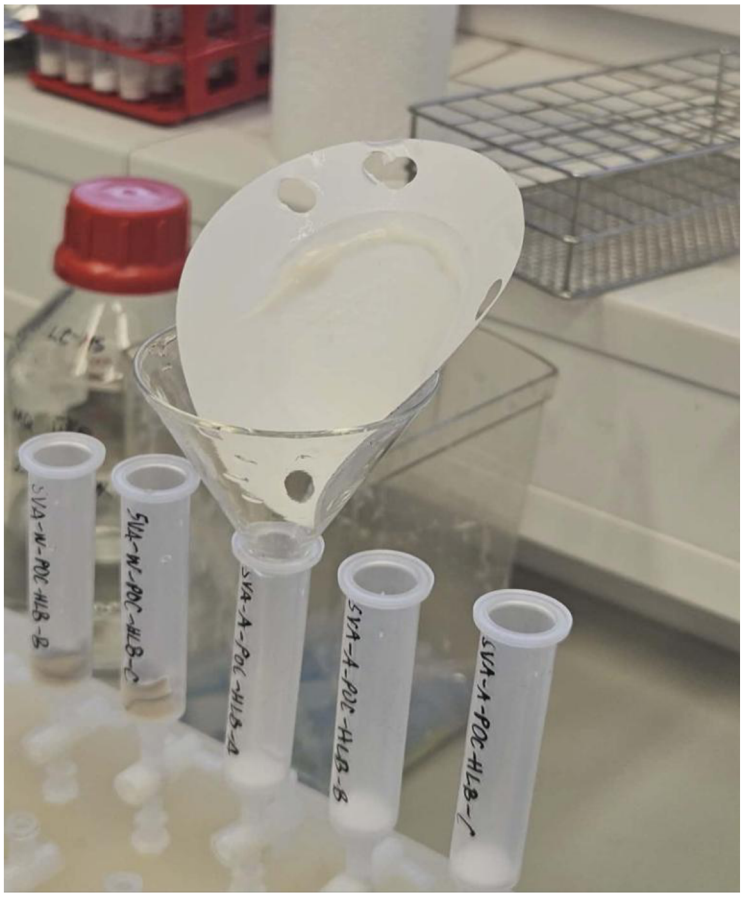

Fig 13: Transfer of sorbent powder from the POCIS-HLB membranes into pre-weighed 6 mL SPE cartridges.

The measured concentrations were first normalized to sorbent mass (ng/g) and then converted to time-weighted water concentrations (ng/L) (Table 3) using compound-specific sampling rates (Rs) at 20 °C and the deployment time, consistent with the recalculation procedure further described in this section.

Tab 3: The calculated Rs (L/day) values for POCIS-HLB and -PFAS samplers.

Compound	**POCIS-HLB (20 °C)**	**POCIS-PFAS (20 °C)**
PFBA	0.00	0.86
PFPeA	0.04	0.13
PFPrS	ND	ND
PFHxA	0.02	0.15
PFBS	0.02	0.21
PFHpA	0.03	0.16
PFPeS	ND	ND
6:2 FTS	0.01	0.17
PFOA	0.06	0.15
PFHxS	0.04	0.22
PFNA	0.07	0.15
PFHpS	0.01	ND
PFOS	0.08	0.17

Time-weighted average water concentrations C*w* (ng/L) were calculated from normalized sorbent concentrations using published sampling rates R*s* (L/day) at 20 °C and the deployment time *t* (days) according to;

$$C_w = \frac{M}{R_s * t}$$

Where, *M* is the accumulated mass on the sorbent (ng).

SPE extraction was performed using a vacuum manifold. An interference wash of 5 mL ultrapure water was applied prior to elution. The analytes were eluted with 2 mL methanol (MeOH), followed by 2 × 2 mL of 0.2% ammonium hydroxide (NH_4OH) in methanol, at a flow rate of approximately 1 drop per second. The combined eluate was evaporated to dryness under a gentle stream of nitrogen prior to analysis. To determine the dry sorbent mass, the loaded SPE cartridges were placed in a desiccator overnight following extraction. Perfluorinated compounds potentially retained on the membranes were additionally extracted by immersing the membranes in methanol.

Quantitative analysis was performed by liquid chromatography tandem mass spectrometry (LC-MS/MS).

Additionally, E & H services (UK) POCIS-HLB was used for passive sampling. The sampler consists of two circular polyethersulfone (PES) membranes that enclose a thin layer of HLB sorbent, onto which dissolved PFAS sorb during deployment. The membranes and sorbent are held together by two rigid metal (stainless steel) frames and sealed with metal rings. During field deployment, water passes through the PES membranes, larger particles are excluded, and target analytes accumulate on the internal HLB sorbent for later extraction and analysis. After field retrieval the HLB was disassembled similar to POCIS-PFAS and SPE extraction was performed using a vacuum manifold. The sorbent is washed with 10 mL of distilled water and the analyte is eluted with 4 × 2 mL LC/MS-grade MeOH.

4.6 PFAS analysis in the Sediment

To analyze PFASs in sediment samples, 50 mg (± 10%) in triplicate was homogenized with the addition of 980 µL of methanol (LC-MS grade, Honeywell) and 20 µL of internal standard mixture of 21 isotopically labelled PFAS (ISTD, 10 ng/mL, Wellington Laboratories, Canada) in a BeadBug microtube homogenizer (D1030-E, Benchmark Scientific) at 4000 rpm for 1 min, repeated 3 times, using 2.8 mm stainless steel beads, followed by incubation overnight at 4°C. The extraction process was further facilitated by subjecting the samples to an ultrasound bath for 30 min at room temperature. Subsequently, each sample was centrifuged at 12,000 rpm for 10 min, and 700 µL of supernatant was separated and transferred into a 1.5 mL polypropylene tube (Eppendorf). Sample purification was carried out using Supelclean ENVI-Carb SPE tube (6 mL, Supelco). Briefly, each sample was acidified with 8 µL of formic acid (LC-MS grade, Sigma-Aldrich) and applied to the conditioned Supelclean ENVI-Carb SPE tube and washed with 10 mL of methanol with 1% formic acid. Preceding the LC-MS analysis, the extracts were evaporated to the volume of 200 µL.

4.7 Instrumental method for PFAS analysis

The samples were then analyzed using an LC-MS/MS system comprising the 1260 Infinity II LC (equipped with 1260 Infinity binary pump) coupled with a 6470 LC/TQ mass spectrometer equipped with an electrospray ionization source (Agilent Jet Stream) operating in both negative and positive mode. The compound separation was achieved using a Zorbax RRHD Eclipse Plus C18 LC column (100 × 3.0 mm, 1.8 µm, Agilent, USA) along with an UHPLC Guard Eclipse Plus C18 precolumn (3.00 mm, 1.8 µm, Agilent, USA). The column was maintained at 45°C, with a 2 µL injection volume and a flow rate changing throughout the gradient programme 0.4-0.8 mL/min.

4.8 Elemental Water analysis and Sediment digestion

In addition to PFAS analyses, the general elemental composition of the waters taken from both locations, i.e., A and W, was also determined, namely cations using inductively coupled plasma optical emission spectrometry (ICP-OES; iCAP 7000

series, Thermo, Germany), total carbon (TC) and total nitrogen (TN) using a TOC-L CPH analyzer equipped with a TNM-L unit (Shimadzu, Kyoto, Japan), and selected anions using a Dionex ICS-5000+ ion chromatography system (Thermo Fisher Scientific, USA) equipped with a conductivity detector. The water samples were not filtered before individual analyses, but diluted with 2% HNO_3 for ICP-OES analysis, or with deionized water for the other mentioned analyses. As the samples were stored in a fridge prior to the analysis without further pre-treatment, and due to the longer time since sampling, only parameters minimally subject to these influences were selected for the results. The results can therefore be considered only approximate, serving mainly for a general comparison of the locations with each other, as will be discussed further.

Finally, to determine the pseudo-total concentration of elements in the sediment from site A, microwave digestion was carried out. Digestion was performed according to EPA 3051A. A 0.5 g portion of previously crushed and homogenized sediment was weighed, and 9 mL HNO_3 and 3 mL HCl were added. The following day, the samples were digested using a Multiwave PRO microwave digestion system (Anton Paar, Germany). After digestion, 1 mL H_2O_2 was added, and the sample was subsequently evaporated to near dryness. It was then re-dissolved in 10 mL of 2% HNO_3, filtered through a 0.45 µm filter, and diluted for ICP-OES measurement. Each sample was digested in triplicate. Concentrations of individual elements were determined using ICP-OES.

5. RESULTS

5.1 GENERAL CHARACTERISTICS OF WATER

A) Cations

The concentration of selected cations in water samples are given in Table 4. The water analysis was performed on samples stored in a refrigerator (without acidification) for 3 months after being collected at the site, as already mentioned in the methodology. With this in mind, these values can only be taken as indicative and serve to differentiate these two locations in direct comparison.

The airport water samples showed low and relatively uniform concentrations of the measured cations across replicates. Ca was the most abundant cation in this sample group, followed by S and Mg, whereas Na and K were present at lower concentrations. Sr showed the lowest concentration and minimal variation among the replicates. Other elements were below the detection of the analytical instrument.

By contrast, the wastewater samples exhibited substantially higher cation concentrations than the airport samples. Na was the dominant cation, with values above 1000 mg/L in all replicates, followed by Mg and S, which also occurred at elevated levels. K was significantly higher in wastewater than in airport water, while Ca remained at a moderate concentration and showed less difference between the two sample types. Sr was the least abundant cation in wastewater, although it was slightly higher than in the airport samples.

Tab 4: Concentration of selected cations in water samples (mg/L).

	Ca mg/L	**K mg/L**	**Mg mg/L**	**S mg/L**	**Na mg/L**	**Sr mg/L**
Airport	77.28 ± 1.96	2.76 ± 1.28	26.54 ± 0.32	86.53 ± 1.87	12.80 ± 0.20	0.56 ± 0.00
Wastewater	72.82 ± 0.04	44.28 ± 0.64	153.56 ± 2.94	152.53 ± 1.09	1092 ± 4.68	1.10 ± 0.00

B) Anions

Table 5 presents the concentrations of chloride (Cl) and bromide (Br) in water samples from the Airport and Wastewater sites. Chloride was detected at both sites, while bromide was not detected (hereafter reported as "ND") in the Airport sample and was only quantified in the Wastewater sample.

Chloride at the Airport site was 11.09 ± 0.84 mg/L, which was markedly lower than the Wastewater site value of 2341 ± 72.5 mg/L, a difference of more than 200-fold. The Wastewater chloride concentration also showed the highest absolute standard deviation of any measurement across both tables (± 72.5 mg/L), indicating considerable variability between replicates. Bromide was measured only in the Wastewater sample at 5.53 ± 0.49 mg/L, with no detectable concentration reported for the Airport sample.

Overall, the data show a clear distinction between the two sample types: the Airport water was characterized by low chloride and non-detectable bromide, whereas the wastewater exhibited very high chloride concentrations and detectable bromide. The remaining anions present in the sample (e.g., sulfates, nitrite, and nitrate) are not presented in the table, since sample storage may have led to changes in their speciation. Therefore, total measured concentrations from ICP-OES, TC, and TN are reported instead. Phosphates and fluorides were below the detection limit in both samples.

Tab 5: Concentration of selected anions in water samples (mg/L).

	Cl **mg/L**	**Br** **mg/L**
Airport	11.09 ± 0.84	ND
Wastewater	2341 ± 72.5	5.53 ± 0.49

C) TOC and TN

The values of total carbon (TC) and total nitrogen (TN) from the Airport and Wastewater are depicted in Table 6. The concentrations of total carbon (TC) and total nitrogen (TN) differed significantly between the airport and wastewater sites (Table 6). At the airport, TC was 16.31 ± 4.34 mg/L, whereas TN was much lower at 0.51 ± 0.03 mg/L. In contrast, the wastewater sample showed a substantially higher TC concentration of 285.16 ± 60.09 mg/L. TN in the wastewater sample was also higher than at the airport, with a mean value of 0.76 ± 1.07 mg/L, although the comparatively large standard deviation indicates greater variability among replicates at this site.

Tab 6: Concentration of TC and TN in water samples (mg/L).

	TC mg/L	**TN mg/L**
Airport	16.31 ± 4.34	0.51 ± 0.03
Wastewater	285.16 ± 60.09	0.76 ± 1.07

5.2 General Characteristics of Sediment

The pseudo-total elemental composition of the sediment samples was provided together with that of Montana soil (reference soil SRM 2710a). The samples were analyzed after digestion with the U.S. EPA Method 3051A using microwave-assisted HNO_3/HCl extraction, as already described in the methodology. This method is widely used for sediment and soil digestion, but it does not fully dissolve silicate minerals. For that reason, the reported concentrations should not be treated as true total concentrations. Instead, they represent a pseudo-total fraction. This means that the results are best used for the comparison between samples, rather than for complete elemental recovery. The obtained results are given in Table 7a and Table 7b.

5.2.1 Major Elements (Al, Fe, Ca, Mg, K, Na, Si)

Iron (Fe) was the element with the highest concentration across all three sites, ranging from 31694 ± 785 mg/kg (site 1) to 36964 ± 2566 mg/kg (site 3), with site 3 showing the highest mean. Aluminum (Al) was elevated and broadly comparable across all three sites: 18224 ± 1276 mg/kg at site 1, 21074 ± 3009 mg/kg at site 2, and 20259 ±

2265 mg/kg at site 3, with site 2 recording the highest mean. The standard deviation at site 3 (± 2265 mg/kg) remained relatively large in proportion to its mean, indicating moderate within-site variability. Silicon (Si) was highest at site 3 (109 ± 4.93 mg/kg) and lowest at site 1 (97.14 ± 8.55 mg/kg), with site 2 intermediate (101 ± 5.40 mg/kg). Calcium (Ca) was consistent across sites 1, 2, and 3: 2452 ± 294, 2436 ± 384, and 2299 ± 47.40 mg/kg, respectively, with site 3 showing the lowest value and least variability. Magnesium (Mg) was similar across all sites (4452 ± 165 at site 1; 4824 ± 338 at site 2; 4712 ± 137 at site 3). Potassium (K) ranged from 3692 ± 275 (site 1) to 4415 ± 764 (site 2) to 4296 ± 673 mg/kg (site 3). Sodium (Na) was 387 ± 7.73 mg/kg at site 1, 472 ± 7.24 mg/kg at site 2, and 376 ± 4.81 mg/kg at site 3, with site 2 showing the highest value.

5.2.2 Trace Metals and Metalloids and Selected Non-metals

Most trace and heavy metal concentrations, including Zn, Cu, Co, Ni, Pb, Sb, and Mn were remarkably consistent across all three sites, with minimal between-site differences and low standard deviations, suggesting a spatially homogeneous distribution and a common sediment source or background input.

Thallium (Tl) also showed marked between-site differences: the highest and most variable concentration occurred at site 2 (54.81 ± 42.21 mg/kg), whereas sites 1 and 3 had lower and less variable values (49.39 ± 16.10 and 29.87 ± 4.34 mg/kg, respectively), with site 3 presenting the lowest and most stable Tl level. Vanadium (V) followed a similar but less pronounced pattern, increasing from 76.16 mg/kg at site 1 to 86.93 mg/kg at site 2 and then slightly decreasing to 82.99 mg/kg at site 3. Lithium (Li) also increased modestly from site 1 to site 3, from 8.80 to 13.29 mg/kg.

Sulfur (S), although not a metal or metalloid, was one of the most abundant non-major elements. Concentrations were high at all sites (1 213-1 510 mg/kg), with site 2 showing both the highest mean (1 510 ± 540 mg/kg) and the largest standard deviation. Phosphorus (P), another non-metal, displayed a clear increasing gradient from site 1 to site 3, with concentrations of 477, 513, and 545 mg/kg, respectively. It was the only element to show such a monotonic trend across the three sites.

The pseudo-total digestion of the Montana soil (SRM 2710a) yielded element concentrations that are systematically lower than the certified total values for most metals. Aluminum, iron, potassium, manganese, sodium, antimony, silicon, strontium, vanadium, and zinc were all under-estimated, typically by factors of about 3-10 compared with the NIST certificate. In contrast, magnesium, calcium, phosphorus, and thallium were closer to the certified concentrations, differing by less than roughly a factor of two. This pattern indicates that the applied digestion procedure recovers only a fraction of the total element inventory in SRM 2710a, consistent with a pseudo-total rather than fully quantitative extraction of the standard soil matrix.

Tab 7a: Pseudo-total concentrations of elements in sediment samples (RS = reference soil).

	Al	B	Ba	Ca	Co	Cr	Cu	Fe	K	Li	Mg
	mg/kg										
RS	12549	21.8	171	13618	6.39	13.12	103	14336	3596	8.11	6016
1	18224 ± 1276	42.19 ± 8.7	103 ± 10.9	2452 ± 294	9.84 ± 0.71	7.85 ± 2.14	21.15 ± 1.14	31694 ± 785	3692 ± 275	8.80 ± 3.02	4452 ± 165
2	21074 ± 3009	42.27 ± 15.70	118 ± 32.82	2436 ± 384	9.66 ± 0.52	10.17 ± 0.96	22.68 ± 1.13	35378 ± 879	4415 ± 764	12.15 ± 2.07	4824 ± 338
3	20259 ± 2265	35.04 ± 2.71	113 ± 5.36	2299 ± 47.40	10.07 ± 0.54	10.77 ± 3.25	22.96 ± 1.14	36964 ± 2566	4296 ± 673	13.29 ± 1.26	4712 ± 137

Tab 7b: Pseudo-total concentrations of elements in sediment samples (RS = reference soil).

	Mn	Na	Ni	P	Pb	S	Sb	Si	Sr	Tl	V	Zn
	mg/kg											
RS	430	170	44.15	517	1031	289	5.99	142	32.85	15.86	23.45	282
1	190 ± 9.20	387 ± 67.73	21.65 ± 0.51	477 ± 18.16	10.12 ± 1.64	1445 ± 177	6.02 ± 0.48	97.14 ± 8.55	71.02 ± 13.08	49.39 ± 16.10	76.16 ± 3.63	61.91 ± 5.41
2	190 ± 13.41	472 ± 67.24	22.85 ± 0.09	513 ± 12.36	9.57 ± 0.47	1510 ± 540	6.26 ± 0.14	101 ± 5.40	76.48 ± 20.77	54.81 ± 42.21	86.93 ± 14.49	64.46 ± 2.63
3	205 ± 17.98	376 ± 74.81	23.31 ± 1.06	545 ± 35.65	10.18 ± 1.15	1213 ± 87.30	6.33 ± 0.18	109 ± 4.93	63.53 ± 7.56	29.87 ± 4.34	82.99 ± 4.97	64.61 ± 3.50

5.3 Laboratory Testing of DGT (Freshwater and Seawater)

The table presented (Table 8) shows how effectively the DGT samplers can extract PFAS from the water samples in the laboratory batch conditions. The DGT performance was measured for four compounds, PFBA, PFBS, PFOA, and PFOS. Experiments were conducted in both freshwater and seawater with a target spiked concentration of 0.5 ppb. The individual concentrations in the table mean: the expected post-spike concentrations (exp c), the concentrations measured after spiking and before DGT sampler deployment (T0), the concentrations measured at sampler retrieval (T1), the concentrations measured after sonication of the bottle to evaluate the possible release of PFAS sorbed to the bottle surface (T2), and the concentration in the gel (c_{DGT}).

Tab 8: Raw experimental measurements and calculated concentration in the DGT gel

Analyte	Matrix	DGT part	c exp (ppb)	Average ± SD c_{DGT} (ppb)	Average ± SD (c T0) (ppb)	Average ±SD (c T1) (ppb)	Average ± SD (c T2) (ppb)
PFBA	Freshwater	DGT gel	0.5	0.41±0.06	0.56 ± 0.07	0.45±0.12	0.36±0.04
PFBA	Sea water	DGT gel	0.5	0.34±0.01	0.03±0.05	0.00±0.00	0.00±0.00
PFBS	Freshwater	DGT gel	0.5	0.26±0.03	0.72±0.03	0.73±0.05	0.71±0.02
PFBS	Sea water	DGT gel	0.5	0.31±0.20	0.71±0.02	0.69±0.04	0.76±0.06
PFOA	Fresh water	DGT gel	0.5	0.47±0.23	0.76±0.05	0.84±0.04	4.34±6.34
PFOA	Seawater	DGT gel	0.5	0.70±0.09	0.73±0.09	0.65±0.01	0.71±0.06
PFOS	Fresh water	DGT gel	0.5	0.31±0.01	0.70±0.15	0.66±0.31	0.58±0.08
PFOS	Sea water	DGT gel	0.5	0.09±0.03	0.36±0.10	0.24±0.01	0.29±0.05

Measured aqueous concentrations at T0, T1, and T2 generally remained within the same order of magnitude as the expected spike concentration, which suggests reasonable stability of the spike throughout the experiment. In freshwater samples,

most concentrations ranged from approximately 0.49 to 0.88 ppb. Some variability was observed across sampling time points. For instance, PFBA freshwater replicate 1 decreased from 0.58 ppb at T0 to 0.37 ppb at T1. This variation may be attributed to analytical uncertainty, minor adsorption to experimental containers, or small losses during sample handling.

An extreme deviation was identified for PFOA in freshwater replicate 1, where the T2 concentration reached 11.66 ppb, exceeding the expected concentration by more than twentyfold. This value is inconsistent with the remainder of the dataset and likely indicates contamination or an analytical error.

In several PFBA seawater samples, measured aqueous concentrations were recorded as zero (or close to zero), resulting in division errors during recovery calculations. These values most likely reflect failed measurements or concentrations below the analytical detection limit.

The c_{DGT} values in the table correspond to the PFAS concentrations recovered from the DGT gel (reported as "recovered" values), which represent the time-integrated labile fraction of PFAS accumulated during deployment. The c_{DGT} values were of the same order of magnitude as the aqueous concentrations but were generally lower. The best agreement was obtained for PFOA in seawater, where c_{DGT} closely matched the solution concentrations, with all values clustering around 0.7 ppb. For PFBA in seawater, c_{DGT} clearly exceeded the essentially zero measured concentrations. In freshwater, c_{DGT} for PFBA fell between the higher T0 and lower T2 concentrations and was close to the nominal spike of 0.5 ppb. For PFBS and PFOS in both matrices, as well as for PFOA in freshwater, c_{DGT} values were consistently lower than the corresponding measured concentrations, typically representing about one-half to one-third of the aqueous values.

The calculated recoveries for individual concentrations, including standard deviations, are given in Table 9. In freshwater, PFBA exhibited an average recovery of 81.89%, indicating good agreement with the expected concentration. PFBS showed a lower recovery of 52.16%, while PFOS showed a moderate recovery of 62.47%. PFOA showed an average recovery of 93.63%, although it exhibited greater variability than the others. In seawater, PFBA recovery decreased to 67.80%, while PFBS recovery averaged 61.89%. PFOA exhibited elevated recoveries, averaging 140.03%, suggesting potential overestimation. PFOS showed the lowest recovery among the compounds in seawater (18.55%), indicating very poor uptake by the DGT gel under saline conditions.

Tab 9: Calculated mean recoveries in seawater and freshwater (green boxes are values within the ideal recovery range, i.e., 60-140%; red values were not available due to the analytical error).

Analyte	Matrix	DGT part	c exp (ppb)	Avg (exp c) (%)	Avg (c T0) (%)	Avg (c T1) (%)	Avg (c T2) (%)	SD (exp c) (%)	SD (c T0) (%)	SD (c T1) (%)	SD (c T2) (%)
PFBA	fresh water	DGT gel	0.5	81.89	74.42	92.66	113.85	12.15	20.98	14.71	26.32
PFBS	fresh water	DGT gel	0.5	52.16	36.35	36.15	36.75	7.69	6.84	7.15	6.17
PFOA	fresh water	DGT gel	0.5	93.63	61.43	55.43	45.97	46.10	30.70	26.06	53.46
PFOS	fresh water	DGT gel	0.5	62.47	45.93	53.68	54.06	2.41	7.34	20.17	7.54
PFBA	sea water	DGT gel	0.5	67.80	N/A	N/A	N/A	2.05	N/A	N/A	N/A
PFBS	sea water	DGT gel	0.5	61.89	43.62	45.61	40.45	40.63	28.20	31.54	24.97
PFOA	sea water	DGT gel	0.5	140.03	97.21	107.75	99.16	18.59	20.62	14.57	11.11
PFOS	sea water	DGT gel	0.5	18.55	28.50	38.69	31.74	6.89	15.25	16.50	8.56

More specifically, the recovery values were compared with concentrations determined at individual stages of the experiment, as already explained. For PFBA and PFOS in seawater, recoveries were already very low at T0 and remained low at T1 and T2, showing that most losses happened immediately after spiking rather than during DGT deployment. For PFBA and PFOS in freshwater, recoveries decreased progressively from T0 to T2, indicating gradual loss from solution over the deployment period with only limited mass recovered after bottle sonication.

PFOA in freshwater showed moderate over-recovery at T0 and T1 but an extreme, highly variable over-recovery at T2, pinpointing strong and uneven sorption to, and release from, bottle walls. In contrast, PFBS in both matrices and PFOA in seawater displayed consistently elevated but stable recoveries across all stages, suggesting a systematic analytical bias rather than stage-specific losses.

Precision of the analytical results was evaluated using the relative standard deviation (RSD), which expresses the spread of replicate measurements relative to their mean and is reported as a percentage (Table 10).

Tab 10: Calculated RSD values in seawater and freshwater.

Analyte	Matrix	DGT part	RSD (exp c) (%)	RSD (c T0) (%)	RSD (c T1) (%)	RSD (c T2) (%)
PFBA	freshwater	DGT gel	12.11	23.02	12.96	18.88
PFBS	freshwater	DGT gel	12.03	15.37	16.14	13.70
PFOA	freshwater	DGT gel	40.20	40.81	38.39	94.96
PFOS	freshwater	DGT gel	3.15	13.05	30.67	11.39
PFBA	seawater	DGT gel	2.47	N/A	N/A	N/A
PFBS	seawater	DGT gel	53.60	52.79	56.47	50.40
PFOA	seawater	DGT gel	10.84	17.32	11.04	9.15
PFOS	seawater	DGT gel	30.31	43.68	34.83	22.03

In freshwater, PFBA and PFBS exhibit low to moderate RSD values across all stages (approximately 12-23%), indicating good repeatability of replicate measurements. PFOA in freshwater presents substantially higher RSDs, around 40% for the expected concentration and for T0-T1, and approaching 95% at T2, where the dispersion among replicates is greatest. PFOS in freshwater shows a low RSD for the expected concentration (3.15%), while RSDs at T0-T2 fall within a moderate range (approximately 11-31%).

In seawater, PFBA displays a very low RSD for the expected concentration (2.47%), whereas RSDs at T0-T2 are not reported because the analyte was not detected. PFBS in seawater is characterized by consistently high RSDs (about 50-56%) at all stages, reflecting pronounced variability between replicates. PFOA in seawater shows low to moderate RSDs, decreasing from 10.84% for the expected concentration to 9.15% at T2. PFOS in seawater exhibits moderate RSDs (approximately 22-44%), with maximal variability at T0 and a progressive decline towards T2.

Overall, recoveries based on expected concentrations cluster roughly around 50-95% in freshwater, except for highly variable PFOA, whereas in seawater they range from very low (PFOS) to moderate (PFBA, PFBS) and highly elevated (PFOA), with several compounds showing large SD and RSD values that indicate high dispersion among replicates. For graphical visualization of the observed trends, the values were plotted in a graph (Fig. 14). Error bars indicate the standard deviation of replicate measurements, and the analytical error in the seawater PFBA T0-T2 calculations is also visible. Horizontal lines at 60% and 140% recovery mark the minimum and

maximum limits used to assess the performance, allowing visual comparison of which compounds and matrices fall within or outside these bounds.

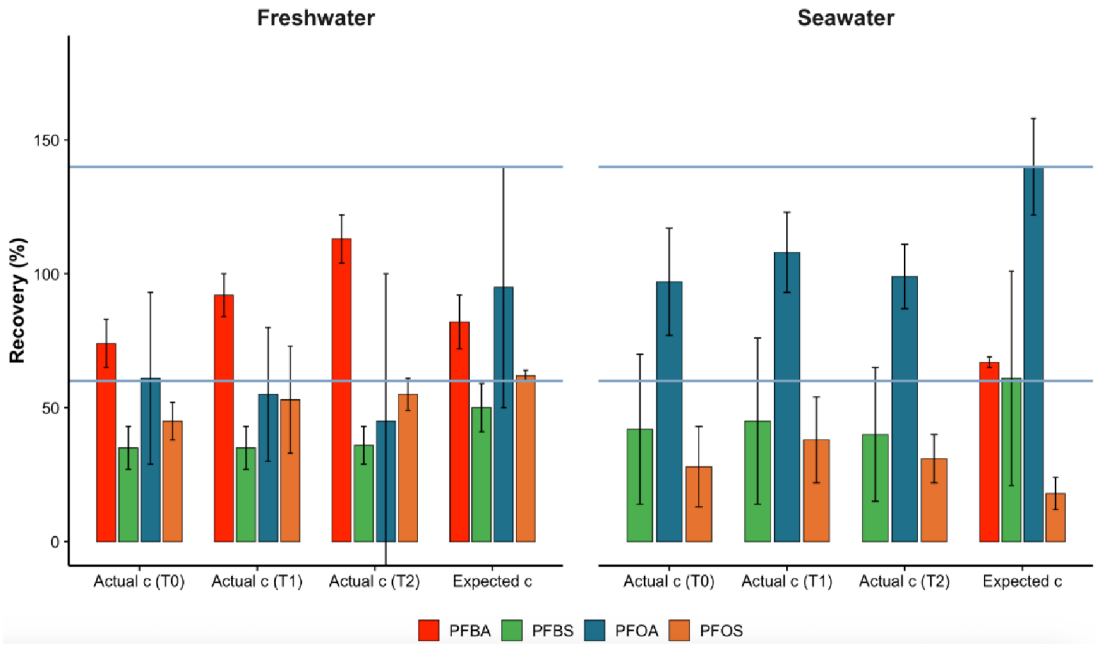

Fig 14: DGT based PFAS recoveries in freshwater and seawater (blue lines showing maximum and minimum recovery %).

Moreover, leaching tests on DGT pistons showed that the sampler bodies were not completely inert to PFAS. For PFBA, PFBS, and PFOA, piston-associated recoveries calculated from the original T0 solution concentration were generally below about 10% in both freshwater and seawater, with most values between roughly 2% and 12%. In contrast, PFOS displayed clearly higher piston recoveries: in freshwater, recoveries were around 30%, while in seawater they ranged from about 80% up to almost 200%, occasionally exceeding the initial PFOS mass present in the system. Solution concentrations at T0-T2 did not show a consistent decrease corresponding to these very high seawater PFOS piston recoveries. This shows that in a closed batch system, the results may be affected by the fact that the DGT pistons are not completely inert.

5.4 Passive samplers from the field

5.4.1 DGT

The recalculated PFAS concentrations measured by DGT samplers at airport and wastewater sites (ng/L) are given in Table 11.

Tab 11: PFAS concentrations measured by DGT samplers at airport and wastewater sites (ng/L).

Compound	Airport (Mean ± SD)	Wastewater (Mean ± SD)
PFBA	2.14 ± 0.47	ND
PFPeA	13.23 ± 3.20	ND
PFHxA	15.22 ± 3.76	ND
PFBS	2.64 ± 1.00	ND
PFHpA	3.39 ± 0.78	ND
PFPeS	2.43 ± 0.38	ND
PFOA	3.38 ± 0.63	ND
PFHxS	16.22 ± 4.31	ND
PFNA	0.00 ± 0.00	ND
PFHpS	0.00 ± 0.00	ND
PFOS	5.44 ± 1.37	ND
SUM	63.08 ± 15.81	ND

DGT samplers deployed at the airport site showed measurable concentrations of eleven PFAS with a mean total concentration of 63.08 ng/L and a standard deviation of 15.81 ng/L. At the airport, the highest mean concentrations were PFHxS (16.22 ng/L), PFHxA (15.22 ng/L), PFPeA (13.23 ng/L), and PFOS (5.44 ng/L), followed by PFHpA (3.39 ng/L), PFOA (3.38 ng/L), PFBS (2.64 ng/L), PFBA (2.14 ng/L), and PFPeS (2.43 ng/L), while PFNA and PFHpS were not detected.
Standard deviations at the airport ranged from 0.38 ng/L (PFPeS) to 4.31 ng/L (PFHxS), with PFPeA and PFHxA also showing relatively high variability (3.20 and 3.76 ng/L, respectively). In wastewater, none of the target PFAS were detected by the DGT samplers.

5.4.2 POCIS-PFAS Sampler

The recalculated PFAS concentrations measured by POCIS-PFAS samplers at airport and wastewater sites (ng/L) are given in Table 12. Since, unlike the DGT sampler, there is no conversion to other temperatures available for POCIS-PFAS, the presented results were calculated for 20°C.

Tab 12: PFAS concentrations measured by POCIS-PFAS samplers at airport and wastewater sites (ng/L).

PFAS	Airport (Mean ± SD)	Wastewater (Mean ± SD)
PFBA	0.50 ± 0.04	ND
PFPeA	14.48 ± 0.95	ND
PFPrS	ND	ND
PFHxA	12.25 ± 0.53	ND
PFBS	2.59 ± 0.19	ND
PFHpA	3.95 ± 0.18	ND
PFPeS	ND	ND
6:2 FTS	0.03 ± 0.06	ND
PFOA	3.80 ± 0.28	ND
PFHxS	11.68 ± 1.03	ND
PFNA	0.15 ± 0.03	ND
PFHpS	ND	ND
PFOS	4.50 ± 0.56	ND
SUM	53.94 ± 3.39	ND

The dominant compounds in POCIS-PFAS at the airport were PFPeA (14.48 ng/L), PFHxA (12.25 ng/L), PFHxS (11.68 ng/L), and PFOS (4.50 ng/L), with lower levels of PFHpA (3.95 ng/L), PFOA (3.80 ng/L), PFBS (2.59 ng/L), and PFBA (0.50 ng/L); 6:2 FTS was present at 0.03 ng/L.Standard deviations at the airport ranged from 0.03-0.06 ng/L for low-level compounds (PFBA, PFNA, 6:2 FTS) up to 1.03 ng/L for PFHxS and 0.95-0.56 ng/L for PFPeA, PFHxA, and PFOS, indicating moderate variability among POCIS replicates. Nevertheless, PFPrS, PFPeS, 6:2 FTS, PFNA, and PFHpS were not detected (ND).

DGT and POCIS showed broadly similar patterns for many PFAS, but DGT tended to yield higher concentrations for several compounds (Fig 15). Across the analytes, DGT reported higher concentrations than POCIS for PFBA, PFHxA, PFHxS, PFPeS, and PFOS, indicating greater accumulated mass for these compounds in the DGT samplers. For PFPeA, PFBS, PFHpA, and PFOA, the two sampler types produced comparable concentrations with overlapping error bars, indicating similar uptake behavior under the experimental conditions. PFNA and PFHpS were near or below detection for both DGT and POCIS, with no evident difference between the two sampling approaches.

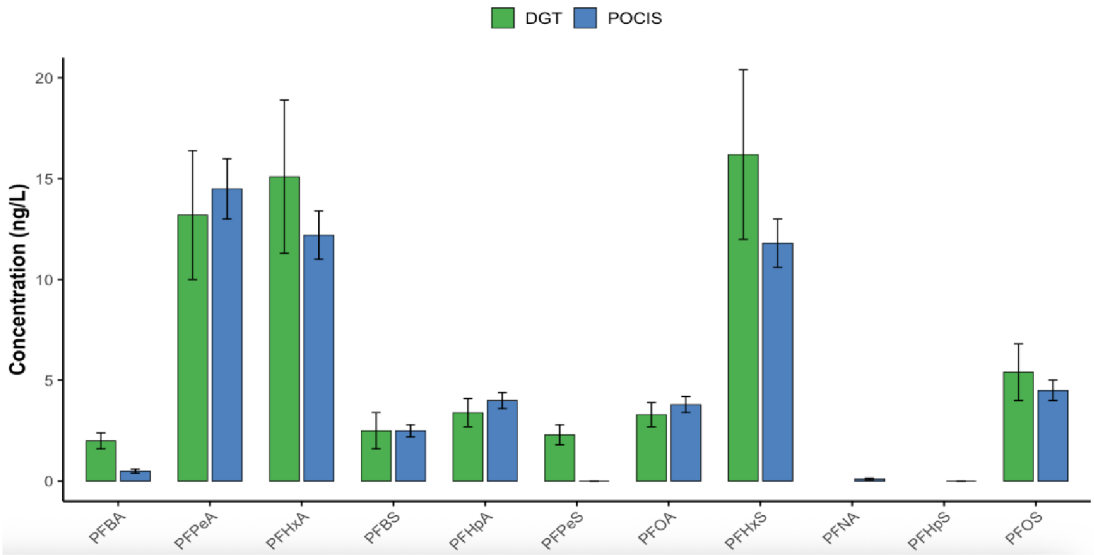

Fig 15: POCIS and DGT measured PFAS at the airport.

5.4.3 POCIS-HLB Sampler

In addition, POCIS-HLB was tested, even though these samplers are not directly for PFAS, but can be used for these compounds. The recalculated PFAS concentrations measured by POCIS-HLB samplers at airport and wastewater sites (ng/L) are given in Table 13. Unlike POCIS-PFAS, POCIS-HLB values can be converted to other temperatures, such as 5°C, which is close to the values measured directly at the site. For this reason, the following table presents the recalculated values for 20°C.

Tab 13: PFAS concentrations measured by POCIS-HLB samplers at airport and wastewater sites (ng/L).

PFAS	Airport (Mean ± SD)	Wastewater (Mean ± SD)
PFBA	0.00 ± 0.00	ND
PFPeA	10.55 ± 0.68	ND
PFPrS	ND	ND
PFHxA	60.70 ± 3.80	ND
PFBS	17.40 ± 1.87	ND
PFHpA	24.27 ± 2.60	ND
PFEeS	ND	ND
6:2 FTS	2.99 ± 0.52	ND
PFOA	12.12 ± 0.41	ND
PFHxS	60.51 ± 17.41	ND
PFNA	0.36 ± 0.03	ND
PFHpS	5.70 ± 3.23	ND
PFOS	1.53 ± 0.93	ND
SUM	196.13 ± 23.42	ND

Across detected compounds at the airport, PFHxA and PFHxS shows the highest mean concentration and the largest standard deviation. PFPeA, PFHpA, PFBS and PFOA form a group with intermediate concentrations (10-25 ng/L). 6:2 FTS and PFOS exhibit lower values, while PFNA is the lowest among the detected PFAS. Several PFAS (PFBA, PFPrS, PFPeS) are either zero or not detected, creating a clear split between detected and non-detected compounds.

5.4.4 Summary of Passive Sampler Results

As already mentioned, for the PFAS-specific POCIS, a wide range of compounds was detected at the airport site, including both short-chain and long-chain perfluoroalkyl acids. Short-chain PFAS such as PFBA and PFPeA were consistently quantified at low ng/L levels, while mid-chain PFCAs (PFHxA, PFHpA, PFOA) and PFSAs (PFBS, PFHxS, PFOS) occurred at several ng/L. Concentrations were relatively balanced, and the overall PFAS pattern was similar to that obtained with DGT samplers, indicating that the PFAS-specific POCIS captured the dissolved PFAS mixture effectively. In contrast, the POCIS-HLB samplers at the airport showed a more restricted and skewed PFAS profile. The PFAS burden was dominated by a few mid- and long-chain analytes, particularly PFHxS, PFHxA, PFHpA, PFPeA, and

PFOA, which together accounted for most of the summed concentration (125.17 ng/L). Among these, PFHxA and PFHxS displayed the highest mean concentration and the largest standard deviation, indicating both a strong contribution to total PFAS and considerable variability among replicates. Other compounds, such as PFHxA, PFBS, and PFOS, were present at intermediate levels, while PFHpS occurred at low ng/L concentrations. Total PFAS concentrations are comparable, with DGT giving a mean concentration of 63.08 ng/L and POCIS 53.94 ng/L, suggesting broadly consistent exposure estimates despite methodological differences. On a compound-by-compound basis, POCIS and DGT differ somewhat in relative contribution. For example, POCIS shows slightly lower PFOS and PFHxS than DGT in terms of share of the total, whereas PFPeA and PFHxA are of similar order in both samplers. From the POCIS-HLB results, it is evident that the PFAS-specific POCIS provides a more comprehensive and compositionally representative measurement of dissolved PFAS, especially for short-chain species, whereas POCIS-HLB underestimates or fails to detect several short-chain PFAS and over-emphasizes selected mid- and long-chain compounds. Both DGT and POCIS samplers show PFAS only at the airport, with no detectable PFAS in the wastewater site for either sampler.

5.5 PFAS Sediments

The concentration of 10 individual PFAS compounds in sediments near the Svalbard airport sampled at the DGT-insertion site is given below (Table 14). For PFAS analysis, sediments collected from three places in the small pond near the airport, where DGT/POCIS samplers were deployed, were measured.

Tab 14: PFAS concentration in sediments near Svalbard airport.

PFAS	Sample 1	Sample 2	Sample 3	Avg ± SD
PFPeA	0.00	0.00	0.00	0.00 ± 0.00
PFHxA	0.00	0.02	0.00	0.01 ± 0.01
PFBS	0.08	0.00	0.22	0.10 ± 0.10
PFHpA	0.05	0.00	0.02	0.02 ± 0.02
PFOA	0.03	0.09	0.06	0.06 ± 0.02
PFHxS	0.09	0.21	0.20	0.17 ± 0.07
PFNA	0.11	0.28	0.26	0.22 ± 0.09
PFDA	0.00	0.01	0.00	0.00 ± 0.00
PFOS	0.30	0.51	0.54	0.45 ± 0.13
PFUnDA	0.00	0.00	0.09	0.03 ± 0.05
PFAS (sum)	0.65	1.12	1.39	1.05 ± 0.37

In this sediment, PFPeA, PFHxA, PFHpA, PFDA, and most PFAS compounds were reported at very low values, while PFOS, PFHxS, PFNA, and PFUnDA contributed most of the measured PFAS load. The PFAS sum increased from 0.65 in sediment 1 to 1.12 in sediment 2 and 1.39 in sediment 3. In sediment 1, the PFAS sum was 0.65, with the highest individual values being PFOS at 0.30, PFHxS at 0.09, and PFNA at 0.11. In sediment 2, the PFAS sum increased to 1.1, and the largest contribution was again PFOS at 0.51, followed by PFNA at 0.28 and PFHxS at 0.21. In sediment 3, the PFAS sum was highest at 1.39, with PFOS at 0.54, PFNA at 0.26, PFHxS at 0.20, and PFUnDA at 0.09. Across all three samples, PFPeA, PFHxA, PFHpA, and PFDAs were reported as 0.0 in at least some samples, and PFHxA and PFPeA were 0.0 in all three samples. PFBS appeared only in sediment 1 and 3, where it was 0.08 and 0.22, respectively, and was 0.0 in sediment 2. PFUnDA was 0.0 in sediments 1 and 2, but 0.09 in sediment 3. Overall, sediment 3 had the highest total PFAS concentration and sediment 1 had the lowest.

6. DISCUSSION

6.1 Laboratory testing of DGT

DGT is widely recognized as one of the robust passive sampling tools particularly when compared to high-frequency grab sampling. The recovery patterns from seawater and freshwater, suggest that the present DGT gel configuration performs best for PFOA and PFBA in freshwater, where mean recoveries are close to or above 80%, while PFBS and PFOS show lower or moderate recoveries, consistent with previous work reporting compound-specific binding efficiencies and chain-length effects in PFAS passive samplers and DGT-type methods (Yang et al., 2022).

The very low PFOS recovery in seawater and the strongly elevated PFOA recovery (around 140%) are consistent with known matrix effects in saline systems, where increased ionic strength and co-occurring anions can alter PFAS speciation, diffusion, and sorption, and can also enhance analytical bias if calibration is not fully matrix-matched. Studies evaluating PFAS with diffusive or equilibrium passive samplers in marine and estuarine waters have similarly reported reduced retention for PFOS and other long-chain sulfonates, together with occasional over-recovery for some carboxylates, such as PFOA, highlighting that method validation must be compound- and matrix-specific (Dunn et al., 2024).Moreover, the high RSD for PFBS in seawater indicates unstable performance for these compounds, which aligns with reports that short-chain PFAS and selected sulfonates can be sensitive to small changes in ionic strength, pH, and competitive sorption on binding gels and resins (Snook et al.,2025; Dunn et al., 2024). Taken together, these results indicate that the current DGT gel setup is more reliable for selected carboxylates in freshwater than for sulfonates, especially PFOS, in seawater, and they underline the need for further optimization of sorbent chemistry, calibration, and quality control when applying DGT to mixed PFAS suites across contrasting water matrices (Dunn et al., 2024; SERDP, 2025), especially in (semi)closed systems such as the one generally designed for laboratory testing of DGT samplers.

The leaching from only the DGT bodies (pistons) were tested, after removing the gel. The results show that the DGT pistons can retain measurable amounts of PFAS, even after removal of the binding gel, confirming that the sampler bodies cannot be considered completely inert. For PFBA, PFBS, and PFOA, the low piston recoveries (mostly ≤10%) indicate only minor sorption to the plastic and construction materials, which is consistent with studies reporting relatively weak interactions of many PFCAs and some short-chain PFAS with sampler housings compared to engineered sorbents (Fang et al., 2021). The substantially higher PFOS recoveries, especially in seawater, suggest that PFOS shows stronger affinity for sampler body materials and internal components than the other tested PFAS, in line with evidence for enhanced sorption of long-chain sulfonates to polymeric surfaces and ancillary sampler materials. Because PFOS concentrations in the aqueous phase did not decrease proportionally

and some apparent piston recoveries exceeded 100%, these body-recovery values likely also include a PFOS-specific analytical or procedural artefact, as has been noted for strongly sorbing PFAS when extraction or volume corrections are imperfect (Medon et al., 2023). Fang et al. (2021) showed, using commercial DGT housings under laboratory conditions, that adsorption of PFAS to DGT pistons and other body components can be non-negligible and compound-specific, with PFOS exhibiting particularly pronounced sorption in some configurations (Fang et al., 2021). Because PFOS concentrations in the aqueous phase did not decrease proportionally and some apparent piston recoveries exceeded 100%, these body-recovery values likely also include a PFOS-specific analytical or procedural artefact, such as incomplete correction for volume changes or desorption from internal surfaces during extraction, which has been noted for strongly sorbing PFAS in both DGT-type and other passive sampling systems (Fang et al., 2021; Snook et al., 2025).

Overall, the piston tests support presenting DGT-derived PFAS data with the caveat that sampler housings may contribute a small background for most PFAS but can cause disproportionately high and potentially biased signals for PFOS, particularly in closed saline systems, which is consistent with current DGT and PFAS passive-sampling literature. This limitation is expected to be less pronounced under field conditions, where larger water volumes and continuous water exchange reduce the relative influence of PFAS retention on the DGT sampler body. In small-volume laboratory batch systems, however, this effect may become non-negligible and should be considered when interpreting the results.

6.2 Field Passive Samplers

In the wider Svalbard region, several studies have documented that waters and other environmental compartments near local PFAS sources are dominated by PFOS, 6:2 FTSA, and PFHxS, whereas more remote or background locations show relatively higher contributions from short-chain PFCAs such as PFBA, PFPeA and PFHxA, reflecting a mixture of local emissions and long-range atmospheric inputs (Flaten et al., 2024). This regional pattern, with sulfonate-rich profiles near AFFF-affected sites and more PFCA-rich signatures in remote snow, freshwater and ice cores, is consistent with broader Arctic observations that replacement of legacy long-chain PFAS has led to increasing proportions of short-chain PFCAs in less impacted areas (Hartz et al., 2024).

The use of passive samplers is particularly advantageous in this context because they integrate exposure over the deployment period and can capture low-level dissolved PFAS that might remain close to or below detection limits in individual grab samples. Several recent studies have shown that tube-type passive samplers and POCIS can resolve spatial and temporal PFAS gradients in Arctic and sub-Arctic waters at low ng/L to pg/L levels, supporting their use for characterizing both local source areas and long-range transport pathways (Dunn et al., 2024; Langberg et al., 2021). The DGT

and POCIS profiles at the Svalbard airport fit this trend by revealing a clear local PFAS signal, even though absolute concentrations are moderate compared to heavily contaminated sites.

The DGT results from the airport indicate a diverse PFAS mixture dominated by mid-chain PFCAs (PFPeA, PFHxA, PFHpA) and PFHxS, with additional contributions from PFOS, PFBA, PFBS and PFOA, while PFNA and PFHpS were below detection. This profile characterized by elevated PFHxS, PFOS and several mid-chain PFCAs, is typical for sites influenced by aqueous film-forming foams (AFFF) and airport activities, where local releases and secondary emissions produce PFAS mixtures rich in sulfonates and C4-C8 carboxylates. The summed DGT-derived PFAS concentration of about 63 ng/L at the airport is within the range reported for surface waters and shallow groundwater near PFAS-impacted airports and firefighting-training sites, although it is lower than the levels observed at the most heavily contaminated facilities in Europe and North America (Ahrens et al., 2024, Dunn et al., 2024).

Against this background, the airport POCIS results in this study show a PFAS profile dominated by PFPeA, PFHxA, PFHxS and PFOS, supporting the interpretation of a mixed local PFAS input rather than a single dominant compound. The presence of shorter-chain PFAS such as PFPeA, PFHxA and PFBA in both DGT and POCIS samplers is in line with previous Svalbard and wider Arctic studies, which have reported that short-chain PFCAs are now common in freshwater, snow and runoff, especially where long-chain PFAS have been substituted by newer formulations (Ahrens et al., 2024; Hartz et al., 2024). Overall, the passive-sampler profiles therefore indicate a mixed PFAS input at the airport site rather than a single dominant compound, combining characteristic AFFF-related sulfonates with mid-chain and short-chain carboxylates, in agreement with other PFAS investigations at airports and military airfields (Filipovic et al., 2014).

In contrast, the DGT wastewater sample showed non-detectable concentrations for all reported compounds. The absence of detectable PFAS in this particular wastewater deployment could indicate genuinely low PFAS levels in the specific effluent at the time of sampling, but it may also reflect field-exposure conditions and sampler sensitivity that were insufficient to accumulate PFAS above method detection limits, as has been observed in other passive-sampling studies at less contaminated or more variable discharge points (Langberg et al., 2021; Hale et al., 2021). This outcome differs from earlier Svalbard wastewater investigations, which reported measurable PFAS concentrations and clear source signatures in airport-associated wastewater, with PFHxS, PFOS and 6:2 FTSA often dominating the ∑PFAS in certain streams (Ahrens et al., 2024). The discrepancy likely reflects differences in sampling location, timing, hydrological conditions and potentially recent changes in AFFF use or wastewater management. Taken together, these findings indicate that airport-related activities remain the main local PFAS source, whereas wastewater signals appear less

stable and may not always be captured by passive samplers under field conditions (Ahrens et al., 2024)

6.2.1 Comparison of DGT and POCIS-PFAS

POCIS-PFAS and DGT produced broadly comparable PFAS concentration profiles at the airport site, while both samplers showed no detectable PFAS at the wastewater site. For the airport, both devices indicated that PFPeA, PFHxA, PFHxS and PFOS were the dominant compounds, with lower but consistent levels of PFBA, PFBS, PFHpA and PFOA, and non-detects for PFNA and PFHpS, which is in line with typical AFFF-related PFAS patterns reported for airport-impacted waters (Gobelius et al., 2019; Ahrens et al., 2024). Summed PFAS concentrations derived from DGT and from POCIS-PFAS were of the same order, suggesting that both samplers captured a similar time-weighted PFAS exposure during the deployment period.

Generally, POCIS results are considered slightly more reliable as a quantitative basis, because PFAS-specific POCIS configurations have been widely calibrated in the laboratory and field, and compound-specific sampling rates (Rs) at 20 °C are available for a wide range of target PFAS (Gobelius et al., 2019; Langberg et al., 2021). However, several studies emphasize that POCIS Rs can vary substantially with temperature, flow and fouling, and that it is difficult to correct these influences in the absence of dedicated Rs temperature relationships or site-specific calibrations (Fang et al., 2021; Medon et al., 2023). In this study, POCIS concentrations were therefore calculated using published 20 °C sampling rates without applying a temperature correction, in contrast to DGT, where diffusion coefficients and Rs can be explicitly adjusted for field temperature via well-defined diffusion–temperature relationships (Fang et al., 2021)

The close agreement between POCIS-PFAS-derived concentrations and temperature-corrected DGT concentrations at the airport site indicates that the two independent passive samplers respond similarly to the PFAS mixture present in this system. For most compounds, differences between POCIS and DGT-derived concentrations are within about 10-20% of the mean, which is comparable to the variability reported in other passive-sampling studies where POCIS and related samplers were benchmarked against grab samples. However, direct quantitative comparisons between POCIS-PFAS and DGT for PFAS remain relatively scarce, and POCIS has so far been more extensively calibrated and field-validated than DGT, including for industrial and wastewater applications (Hale et al., 2021; Langberg et al., 2021). This level of agreement therefore supports the use of DGT as a complementary method to POCIS-PFAS for characterizing PFAS contamination in cold, remote surface waters (Hale et al., 2021; Fang et al., 2021).

6.3 PFAS Sediments

The PFAS concentrations measured in airport sediments across the three samples, showed PFOS as the consistently dominant compound. The sampling location at the

airport, where firefighting foam use is an established activity, provides a direct potential source for the observed PFAS pattern. These concentrations are above the background levels reported for marine sediments from unaffected Norwegian areas, where surface sediment PFAS sums were generally below 0.5 ng/g dw (Boitsov et al., 2025).

The dominance of PFOS across all three sediment samples is directly consistent with AFFF-derived contamination. Legacy AFFF formulations used at airports historically contained high proportions of PFOS and its precursors, which are released during firefighting training and emergency operations and subsequently accumulate in adjacent soils and sediments (Ahrens et al., 2015). At Stockholm Arlanda Airport, PFOS contributed approximately 86% of total PFAS in sediment near the fire training area, a pattern attributed explicitly to historical AFFF use (Ahrens et al., 2015). In a Norwegian Arctic fjord near an airport, PFOS similarly dominated at the airport-influenced sampling station and accounted for 45% of total PFAS, while background stations were dominated by long-chain PFCAs instead (Ali et al., 2021). The preferential accumulation of PFOS in sediment is further explained by its strong sorption affinity for sediment particles, which increases with fluorocarbon chain length and is significantly greater for sulfonates than for carboxylates of equivalent chain length (Higgins and Luthy, 2006).

The detection of PFHxS across all three sediment samples also reflects an AFFF source signature. Certain AFFF formulations, particularly those developed as substitutes after PFOS restrictions, contain elevated proportions of PFHxS (Skaar et al., 2019). At firefighting training sites on Svalbard, Skaar et al. (2019) identified PFOS as the dominant compound at AFFF-impacted locations, with PFHxS also present, and noted that the PFAS composition at training sites differed clearly from background and landfill locations. Johansson Blomér (2017) reported that both PFOS and PFHxS were the primary compounds in sediment adjacent to a military airport fire drill area in Sweden, supporting the view that co-occurrence of these two sulfonates is a characteristic fingerprint of AFFF-impacted sediments.

The PFAS profile in the airport sediments, dominated by PFOS and PFHxS with only minor contributions from mid-chain PFCAs, contrasts with the more mixed pattern observed in the water column by passive samplers, where PFPeA, PFHxA and other shorter-chain PFCAs contribute a larger share of ∑PFAS. This difference is consistent with previous airport and fire-training studies showing that long-chain sulfonates have higher sediment-water partition coefficients and stronger sorption to organic matter and mineral surfaces than shorter-chain PFCAs, leading to PFOS-enriched sediment profiles even where the overlying water contains a broader AFFF-related mixture (Higgins and Luthy, 2006; Ahrens et al., 2024). Taken together, the combined sediment and passive-sampler data indicate that the pond acts as a long-term sink for PFOS and PFHxS, while more mobile mid- and short-chain acids remain

comparatively enriched in the dissolved phase and are better captured by the passive samplers.

The gradual increase in total PFAS from sediment 1 (0.65 ng/g dw) to sediment 3 (1.39 ng/g dw) most likely reflects small-scale heterogeneity in PFAS distribution within this small pond, rather than a systematic gradient in distance from a primary source area at the airport (Boitsov et al., 2025). Sediment core data from the fjord adjacent to Flesland Airport in Bergen showed a continuous increase in PFAS concentrations since at least the 1980s, with concentrations and precursor loads highest closest to the airport, consistent with a long-term legacy of AFFF-derived contamination accumulating in proximal sediments (Boitsov et al., 2025). Although the concentrations in the present study are considerably lower than those at the most heavily impacted fire training sites, the PFAS profile, dominated by PFOS and PFHxS with contributions from mid-chain PFCAs, is characteristic of AFFF influence and distinguishable from background or long-range transport patterns (Ahrens et al., 2015; Skaar et al., 2019; Ahrens et al., 2024).

CONCLUSION

This thesis provides a multi-matrix assessment of PFAS contamination in the vicinity of Longyearbyen, Svalbard, combining passive water sampling, sediment analysis, and elemental characterisation at two environmentally distinct sites. PFAS were detected at the AFFF-impacted airport site across all three sampling approaches, with DGT and POCIS-PFAS yielding broadly comparable summed dissolved concentrations of 63.08 and 53.94 ng/L, respectively, dominated by PFHxS, PFHxA, PFPeA, and PFOS. Sediment analysis confirmed PFOS as the dominant compound (mean 0.45 ng/g dw), with total PFAS sums ranging from 0.65 to 1.39 ng/g dw, a profile characteristic of legacy AFFF contamination. No PFAS were detected at the wastewater site by any sampler, highlighting the localised nature of the contamination signal and the contrasting influence of site-specific water chemistry, particularly the approximately ten-fold difference in conductivity between the two sites.

From a methodological standpoint, the laboratory evaluation demonstrated that DGT performance is compound- and matrix-specific: recoveries were acceptable for PFBA and PFOA in freshwater (82% and 94%, respectively), but substantially lower for PFOS in seawater (19%), reflecting the influence of ionic strength and chain-length-dependent sorption behaviour. The close agreement between DGT and POCIS-PFAS concentrations in the field, with differences generally within 10-20% for most compounds, supports the use of DGT as a complementary passive sampling tool in Arctic surface waters. POCIS-HLB, while able to detect a broader PFAS sum, showed a skewed profile that underrepresented short-chain compounds and over-emphasised selected mid- and long-chain analytes, reinforcing the importance of sorbent-specific selection when monitoring complex PFAS mixtures.

In a broader context, this work demonstrates that PFAS contamination at Svalbard Airport is driven primarily by local AFFF-related sources, producing a dissolved PFAS mixture of sulfonates and mid-chain perfluorocarboxylates in the water column and preferential enrichment of long-chain sulfonates in sediment; a pattern consistent with other AFFF-impacted airports and fire-training sites internationally. The data generated serve as a baseline for assessing remediation progress at the airport site and contribute to the growing methodological evidence base for time-integrated PFAS monitoring in remote polar environments, where logistical constraints and low dissolved concentrations make passive sampling particularly valuable. As climate change accelerates permafrost thaw and glacial retreat, the remobilisation of historically stored PFAS in the cryosphere is expected to intensify, further underlining the need for sustained, multi-method surveillance in Arctic settlements such as Longyearbyen.

BIBLIOGRAPHY AND SOURCES USED

Scientific books

Huckins, J. N., Petty, J. D., and Booij, K., 2006: Monitors of organic chemicals in the environment: semipermeable membrane devices. Springer, New York.

Article in a scientific periodical

Ahrens, L., Rakovic, J., Ekdahl, S., Kallenborn, R., 2023: Environmental distribution of per- and polyfluoroalkyl substances (PFAS) on Svalbard: local sources and long-range transport to the Arctic. Chemosphere, 345. 140463.

Ahrens, L., Norström, K., Viktor, T., Palm Cousins, A., Josefsson, S., 2015: Stockholm Arlanda Airport as a source of per- and polyfluoroalkyl substances to water, sediment and fish. Chemosphere, 129. 33-38.

Alvarez, D. A., Petty, J. D., Huckins, J. N., Jones-Lepp, T. L., Getting, D. T., Goddard, J. P., Manahan, S. E., 2004: Development of a passive, in situ, integrative sampler for hydrophilic organic contaminants in aquatic environments. Environmental Toxicology and Chemistry, 23(7). 1640-1648.

AMAP, 2014: Trends in Stockholm Convention persistent organic pollutants (POPs) in Arctic air, human media and biota. AMAP Technical Report No. 7 (2014). Arctic Monitoring and Assessment Programme (AMAP), Oslo, Norway. 54 pp.

AMAP, 2017: AMAP Assessment 2016: chemicals of emerging Arctic concern. Arctic Monitoring and Assessment Programme (AMAP), Oslo, Norway. xvi+353 pp.

AMAP, 2017: Chemicals of emerging Arctic concern: summary for policy-makers. Arctic Monitoring and Assessment Programme (AMAP), Oslo, Norway. 16 pp.

AMAP, 2017: Snow, water, ice and permafrost in the Arctic (SWIPA) 2017. Arctic Monitoring and Assessment Programme (AMAP), Oslo, Norway. xiv+269 pp.

Armitage, J. M., MacLeod, M., Cousins, I. T., 2009: Modeling the global fate and transport of perfluorooctanoic acid (PFOA) and perfluorooctanoate (PFO) emitted from direct sources using a multispecies mass balance model. Environmental Science & Technology, 43. 1134-1140.

Arulananthan, M., et al., 2025: Per- and polyfluoroalkyl substances (PFAS) in the cryosphere: occurrence, organismic accumulation, ecotoxicological impacts, transformation, and management strategies. Frontiers in Environmental Science, 13. 1559941.

Boitsov, S., Bruvold, A., Hanssen, L., Jensen, H. K. B., Ali, A., 2024: Per- and polyfluoroalkyl substances (PFAS) in surface sediments of the North-east Atlantic Ocean: a non-natural PFAS background. Environmental Advances, 16. 100545.

Buck, R. C., Franklin, J., Berger, U., Conder, J. M., Cousins, I. T., de Voogt, P., Jensen, A. A., Kannan, K., Mabury, S. A., van Leeuwen, S. P. J., 2011: Perfluoroalkyl and polyfluoroalkyl substances in the environment: terminology,

classification, and origins. Integrated Environmental Assessment and Management, 7(4). 513-541.

Fang, Z., Li, Y., Li, Y., Yang, D., Zhang, H., Jones, K. C., Gu, C., Luo, J., 2021: Development and applications of novel DGT passive samplers for measuring 12 per- and polyfluoroalkyl substances in natural waters and wastewaters. Environmental Science & Technology, 55(14). 9548-9556.

Davison, W., Zhang, H., 1994: In situ speciation measurements of trace components in natural waters using thin-film gels. Nature, 367(6463). 546-548.

D'eon, J. C., Crozier, P. W., Furdui, V. I., Reiner, E. J., Libelo, E. L., Mabury, S. A., 2009: Perfluorinated phosphonic acids in Canadian surface waters and wastewater treatment plant effluent: discovery of a new class of perfluorinated acids. Environmental toxicology and chemistry, 28(10). 2101-2107.

Duan, Q., Duan, L., Liu, Y., Naidu, R., Zhang, H., Lei, Y., 2020: A novel in-situ passive sampling technique in the application of monitoring diuron in the aquatic environment. Environmental Technology & Innovation, 20. 101073.

Dunn, M., Vojta, S., Soltwedel, T., von Appen, W.-J., Lohmann, R., 2024: Passive sampler-derived profiles and mass flows of Perfluorinated Alkyl Substances (PFASs) in surface waters of the Fram Strait. Environmental Science & Technology Letters, 11(2). 166-171.

EFSA Panel on Contaminants in the Food Chain (EFSA CONTAM Panel)., 2020: Risk to human health related to the presence of perfluoroalkyl substances in food. EFSA Journal, 18(9). E06223.

Filipovic, M., Woldegiorgis, A., Norström, K., Bibi, M., Lindberg, M., & Österås, A.-H. (2015). Historical usage of aqueous film forming foam: a case study of the widespread distribution of perfluoroalkyl acids from a military airport to groundwater, lakes, soils and fish. Chemosphere, 129, 39-45.

Førland, E. J., Benestad, R., Hanssen-Bauer, I., Haugen, J. E., Skaugen, T., 2011: Temperature and precipitation development at Svalbard 1900-2100. Norwegian Meteorological Institute Report 03/2011. Norwegian Meteorological Institute, Oslo.

Gao, L., Gao, B., Xu, D., and Liu, L., 2020: DGT: a promising technology for in-situ measurement of metal speciation in the environment. Science of The Total Environment, 715, 136810.

Gardiner, C., Robuck, A., Becanova, J., Cantwell, M., Kaserzon, S., Katz, D., Mueller, J., Lohmann, R., 2022: Field validation of a novel passive sampler for dissolved per- and polyfluoroalkyl substances (PFAS) in surface waters. Environmental Toxicology and Chemistry, 41(10). 2375-2385.

Gobelius, L., Persson, C., Wiberg, K., Ahrens, L., 2019: Calibration and application of passive sampling for per- and polyfluoroalkyl substances in a drinking water treatment plant. Journal of Hazardous Materials, 362. 230-237.

Grünberg, I., Groenke, B., Westermann, S., Boike, J., 2024: Permafrost and active layer temperature and freeze/thaw processes at Svalbard. Journal of Geophysical Research: Earth Surface, 129. e2024JF007648.

Gwynn, J. P., Dowdall, M., Davids, C., Selnæs, Ø. G., Lind, B., 2004: The radiological environment of Svalbard. Polar Research, 23(2). 167-180.

Hale SE, Canivet B, Rundberget T, Langberg HA., Allan IJ., 2021: Using Passive Samplers to Track per and Polyfluoroalkyl Substances (PFAS) Emissions From the Paper Industry: Laboratory Calibration and Field Verification. Front. Environ. Sci. 9:796026.

Joerss, H., Xie, Z., Wagner, C. C., von Appen, W.-J., Sunderland, E. M., Ebinghaus, R., 2020: Transport of legacy Perfluoroalkyl Substances and the Replacement Compound HFPO-DA through the Atlantic Gateway to the Arctic Ocean-Is the Arctic a Sink or a Source?. Environmental Science & Technology, 54(16). 9958-9967.

Kwok, K. Y., Yamazaki, E., Yamashita, N., Taniyasu, S., Murphy, M. B., Horii, Y., Petrick, G., Kallerborn, R., Kannan, K., Murano, K., & Lam, P. K., 2013: Transport of perfluoroalkyl substances (PFAS) from an arctic glacier to downstream locations: implications for sources. The Science of the total environment, 447. 46-55.

Langberg, H. A., Arp, H. P. H., Breedveld, G. D., Slinde, G. A., Høiseter, Å., Grønning, H. M., Jenssen, B. M., 2021: Paper product production identified as the main source of PFAS in a Norwegian lake: source and historic emission tracking. Environmental Pollution, 273. 116259.

Liestøl, O., 1993: Glaciers of Svalbard, Norway. U.S. Geological Survey Professional Paper 1386-E. U.S. Geological Survey, Reston, VA.

Lohmann, R., Abass, K., Bonefeld-Jørgensen, E. C., Bossi, R., Dietz, R., Ferguson, S., Fernie, K. J., Grandjean, P., Herzke, D., Houde, M., Lemire, M., Letcher, R. J., Muir, D., De Silva, A. O., Ostertag, S. K., Rand, A. A., Søndergaard, J., Sonne, C., Sunderland, E. M., Vorkamp, K., Wilson, S., Weihe, P., 2024: Cross-cutting studies of per- and polyfluorinated alkyl substances (PFAS) in Arctic wildlife and humans. The Science of the total environment, 954. 176274.

McConnell. J.R., R. Edwards., 2008: Coal burning leaves toxic heavy metal legacy in the Arctic, Proc. Natl. Acad. Sci. U.S.A. 105 (34) 12140-12144.

Medon, B., Pautler, B. G., Sweett, A., Roberts, J., Risacher, F. F., 2023: A field-validated equilibrium passive sampler for the monitoring of per- and polyfluoroalkyl substances (PFAS) in sediment pore water and surface water. Environmental Science: Processes & Impacts, 25. 980-995.

Meegoda, J. N., Kewalramani, J. A., Li, B., Marsh, R. W., 2020: A Review of the Applications, Environmental Release, and Remediation Technologies of Per- and Polyfluoroalkyl Substances. International Journal of Environmental Research and Public Health, 17(21). 8117.

Muir, D. C. G., Gunnarsdóttir, M. J., Koziol, K., von Hippel, F. A., Szumińska, D., Ademollo, N., Corsolini, S., De Silva, A. O., Gabrielsen, G., Kallenborn, R., Polkowska, Ż., Krümmel, E., Vorkamp, K., 2025: Local sources versus long-range transport of organic contaminants in the Arctic: future developments related to climate change. Environmental Science: Advances, 4(3). 355-408.

Müller, C. E., De Silva, A. O., Small, J., Williamson, M., Wang, X., Morris, A., Katz, S., Gamberg, M., Muir, D. C., 2011: Biomagnification of perfluorinated compounds in a remote terrestrial food chain: lichen-caribou-wolf. Environmental Science & Technology, 45(20). 8665-8673.

Nahar, K., Zulkarnain, N. A., Niven, R. K., 2023: A review of analytical methods and technologies for monitoring PFAS in water. Water, 15(20). 3577.

Okazoe, T., 2009: Overview on the history of organofluorine chemistry from the viewpoint of material industry. Proceedings of the Japan Academy, Series B, 85(8). 276-289.

Ottesen, R. T., Langedal, M., 2001: Urban geochemistry in Trondheim, Norway. NGU Bulletin, 438. 63-69.

Prevedouros, K., Cousins, I. T., Buck, R. C., Korzeniowski, S. H., 2006: Sources, fate and transport of perfluorocarboxylates. Environmental Science & Technology, 40(1). 32-44.

Roos, A. M., Gamberg, M., Muir, D., et al., 2022: Perfluoroalkyl substances in circum-Arctic Rangifer: caribou and reindeer. Environmental Science and Pollution Research, 29. 23721-23735.

Skaar, J. S., Raeder, E. M., Lyche, J. L., et al., 2019: Elucidation of contamination sources for poly- and perfluoroalkyl substances (PFASs) on Svalbard (Norwegian Arctic). Environmental science and pollution research international, 26(8). 7356-7363.

Snook, J., Becanova, J., Vojta, S., Lohmann, R., 2025: Furthering the Capabilities of Diffusive-Gradient Passive Samplers for Per- and Polyfluoroalkyl Substances. Environmental Science & Technology, 59(19). 9744-9753.

Spolaor, A., Scoto, F., Larose, C., Barbaro, E., Burgay, F., Bjorkman, M. P., Cappelletti, D., Dallo, F., de Blasi, F., Divine, D., Dreossi, G., Gabrieli, J., Isaksson, E., Kohler, J., Martma, T., Schmidt, L. S., Schuler, T. V., Stenni, B., Turetta, C., Luks, B., Casado, M., Gallet, J.-C., 2024: Climate change is rapidly deteriorating the climatic signal in Svalbard glaciers. The Cryosphere, 18(1). 307-320.

Vidal, A., Babut, M., Garric, J., Beaudouin, R., 2019: Elucidating the fate of perfluorooctane sulfonate using a rainbow trout (Oncorhynchus mykiss) physiologically based toxicokinetic model. Science of The Total Environment, 691. 1297-1309.

Vrana, B., Allan, I. J., Greenwood, R., Mills, G. A., Dominiak, E., Svensson, K., Knutsson, J., Morrison, G., 2005: Passive sampling techniques for monitoring pollutants in water. TrAC Trends in Analytical Chemistry, 24(10). 845-868.

Wang, Z., Cousins, I. T., Scheringer, M., Buck, R. C., Hungerbühler, K., 2014: Global emission inventories for C4-C14 perfluoroalkyl carboxylic acid homologues from 1951 to 2030, part I: production and emissions from quantifiable sources. Environment International, 70. 62-75.

Wania, F., Mackay, D., 1996: Tracking the distribution of persistent organic pollutants. Environmental Science & Technology, 30(9). 390A-396A.

Hartz, W. F., Björnsdotter, M. K., Yeung, L. W. Y., Humby, J. D., Eckhardt, S., Evangeliou, N., Ericson Jogsten, I., Kärrman, A., Kallenborn, R., 2024: Sources and seasonal variations of per- and polyfluoroalkyl substances (PFAS) in surface snow in the Arctic. Environmental Science & Technology, 58(49). 21817-21828.

Yang, Y., Liu, S., Wang, R., Li, C., Tang, J., Chen, T., Ying, G. G., Chen, C. E., 2022: Diffusive gradients in thin films (DGT) probe for effectively sampling of per- and polyfluoroalkyl substances in waters and sediments. Journal of environmental sciences (China), 121. 90-97.

Yao, Y., Sun, Q., Wang, C., Wang, P.-F., Miao, L.-Z., Ding, S.-M., 2016: The Combination of DGT Technique and Traditional Chemical Methods for Evaluation of Cadmium Bioavailability in Contaminated Soils with Organic Amendment. International Journal of Environmental Research and Public Health, 13(6). 595.

Zenobio, J., Salawu, O., Han, Z., Adeleye, A., 2022: Adsorption of per- and polyfluoroalkyl substances (PFAS) to containers. Journal of Hazardous Materials Advances, 7. 100130.

Zhang, H., Davison, W., Knight, B., McGrath, S., 1998: In situ measurements of solution concentrations and fluxes of trace metals in soils using DGT. Environmental Science & Technology, 32(5). 704-710.

Zhang, H., Davison, W., 1995: Performance characteristics of diffusion gradients in thin films for the in situ measurement of trace metals in aqueous solution. Analytical Chemistry, 67(19). 3391-3400.

Internet source – monograph, article on web portal

DGT Research Ltd., 2022: LSNW-AP Loaded DGT device for PFCs in solutions (on-line). [cit. 2026.03.28], available at <https://www.dgtresearch.com/wp-content/uploads/2022/03/DGT-method-LSNW-AP-website-feb-converted.pdf>.

Internet source – websites of institutions, municipalities

California State Water Quality Control Board, 2020: Per- and Polyfluoroalkyl Substances (PFAS) Sampling Guidelines for Non-Drinking Water (on-line). [cit. 2026.03.28], available at <https://www.waterboards.ca.gov/pfas/docs/sept_2020_pfas_sampling_guidelines.pdf>.

DGT Research Ltd., 2022: LSNW-AP Loaded DGT device for PFCs in solutions (on-line). [cit. 2026.03.28], available at <https://www.dgtresearch.com/wp-content/uploads/2022/03/DGT-method-LSNW-AP-website-feb-converted.pdf>.

New Jersey Department of Environmental Protection, 2021: PFAS Sampling Information for Water Systems Performing Sample Collection (on-line). [cit. 2026.02.08], available at <https://www.nj.gov/dep/watersupply/pdf/pfna-pfas-sampling-guidance-for-nj-water-systems.pdf>.

Secretariat of the Stockholm Convention, 2025: Stockholm Convention on Persistent Organic Pollutants (POPs): Text and Annexes. Revised in 2025 (on-line). [cit. 2026.02.08], available at <https://chm.pops.int/Portals/0/download.aspx?e=UNEP-POPS-COP-CONVTEXT-2025.English.pdf>.

Secretariat of the Stockholm Convention, 2019: SC-9/12: Listing of perfluorooctanoic acid (PFOA), its salts and PFOA-related compounds (on-line). [cit. 2026.02.08], available at <https://www.pops.int/Portals/0/download.aspx?d=UNEP-POPS-COP.9-SC-9-12.English.pdf>.

Secretariat of the Stockholm Convention, 2019: SC-9/4: Perfluorooctane sulfonic acid, its salts and perfluorooctane sulfonyl fluoride (on-line). [cit. 2026.02.08], available at <https://www.pops.int/Portals/0/download.aspx?d=UNEP-POPS-COP.9-SC-9-4.English.pdf>.

U.S. Environmental Protection Agency, 2006: 2010/2015 PFOA Stewardship Program – Guidance on Reporting Emissions and Product Content (on-line). [cit. 2026.02.07], available at <https://www.epa.gov/assessing-and-managing-chemicals-under-tsca/fact-sheet-20102015-pfoa-stewardship-program>.

U.S. Environmental Protection Agency, 2017: Per- and Polyfluoroalkyl Substances (PFAS): Sampling Studies and Methods Development for Water and Other Environmental Media (on-line). EPA/600/F-17/022. [cit. 2026.02.07], available at <https://www.epa.gov/water-research/pfas-analytical-methods-development-and-sampling-research>.

U.S. Environmental Protection Agency, 2019: Method 533: Determination of Per- and Polyfluoroalkyl Substances in Drinking Water by Isotope Dilution Anion Exchange Solid Phase Extraction and Liquid Chromatography/Tandem Mass Spectrometry (on-line). EPA 815-B-19-020. [cit. 2026.02.07], available at <https://www.epa.gov/dwanalyticalmethods/method-533-determination-and-polyfluoroalkyl-substances-drinking-water-isotope>.

U.S. Environmental Protection Agency, 2020: Method 537.1: Determination of Selected Per- and Polyfluorinated Alkyl Substances in Drinking Water by Solid Phase Extraction and Liquid Chromatography/Tandem Mass Spectrometry (LC/MS/MS). Version 2.0 (on-line). EPA/600/R-20/006. [cit. 2026.02.07], available at <https://nepis.epa.gov/Exe/ZyNET.exe/P10111J4.TXT?ZyActionD=ZyDocument&Client=EPA&Index=2016+Thru+2020&Docs=&Query=&Time=&EndTime=&SearchMethod=1&TocRestrict=n&Toc=&TocEntry=&QField=&QFieldYear=&QFieldMonth=&QFieldDay=&IntQFieldOp=0&ExtQFieldOp=0&XmlQuery=&File=D%3A%5Czyfiles%5CIndex%20Data%5C16thru20%5CTxt%5C00000022%5CP10111J4.txt&User=ANONYMOUS&Password=anonymous&SortMethod=h%7C-&MaximumDocuments=1&FuzzyDegree=0&ImageQuality=r75g8/r75g8/x150y150

g16/i425&Display=hpfr&DefSeekPage=x&SearchBack=ZyActionL&Back=ZyActionS&BackDesc=Results%20page&MaximumPages=1&ZyEntry=1&SeekPage=x&ZyPURL>.